

Review

Structural biology of bacterial iron uptake

Karla D. Krewulak, Hans J. Vogel*

Structural Biology Research Group, Department of Biological Sciences, University of Calgary, Calgary, Alberta, Canada T2N 1N4

Received 27 April 2007; received in revised form 20 July 2007; accepted 24 July 2007

Available online 19 August 2007

Abstract

To fulfill their nutritional requirement for iron, bacteria utilize various iron sources which include the host proteins transferrin and lactoferrin, heme, and low molecular weight iron chelators termed siderophores. The iron sources are transported into the Gram-negative bacterial cell via specific uptake pathways which include an outer membrane receptor, a periplasmic binding protein (PBP), and an inner membrane ATP-binding cassette (ABC) transporter. Over the past two decades, structures for the proteins involved in bacterial iron uptake have not only been solved, but their functions have begun to be understood at the molecular level. However, the elucidation of the three dimensional structures of all components of the iron uptake pathways is currently limited. Despite the low sequence homology between different bacterial species, the available three-dimensional structures of homologous proteins are strikingly similar. Examination of the current three-dimensional structures of the outer membrane receptors, PBPs, and ABC transporters provides an overview of the structural biology of iron uptake in bacteria.

© 2007 Elsevier B.V. All rights reserved.

Keywords: Structure; Iron; Heme; Bacterial iron uptake

Contents

1. Introduction	1781
2. Transferrin/lactoferrin	1783
3. Heme as an iron source	1784
4. Siderophores	1787
4.1. Outer membrane receptors	1787
4.1.1. β -barrel domain	1787
4.1.2. Cork domains	1789
4.2. Periplasmic siderophore binding proteins	1792
5. TonB–ExbB–ExbD	1795
6. ATP-binding cassette transporters	1797
7. Conclusions	1800
Note added in proof	1800
Acknowledgements	1800
References	1800

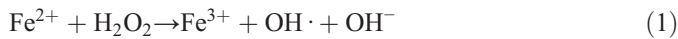
1. Introduction

Iron is an important micronutrient for virtually all living organisms except lactic acid bacteria where manganese and cobalt are used in place of iron [1]. Under physiological

* Corresponding author. Tel.: +1 403 220 6006; fax: +1 403 289 9311.
E-mail address: vogel@ucalgary.ca (H.J. Vogel).

conditions, iron can exist in either the reduced ferrous (Fe^{2+}) form or the oxidized ferric (Fe^{3+}) form. The redox potential of $\text{Fe}^{2+}/\text{Fe}^{3+}$ makes iron extremely versatile when it is incorporated into proteins as a catalytic center or as an electron carrier [2–5]. Thus iron is important for numerous biological processes which include photosynthesis, respiration, the tricarboxylic acid cycle, oxygen transport, gene regulation, DNA biosynthesis, etc.

Although iron is abundant in nature, it does not normally occur in its biologically relevant ferrous form. Under aerobic conditions, the ferrous ion is unstable. Via the Fenton reaction, ferric ion and reactive oxygen species are created, the latter of which can damage biological macromolecules [6,7].



The ferric ion aggregates into insoluble ferric hydroxides. Because of iron's reactivity, it is sequestered into host proteins such as transferrin, lactoferrin, and ferritin. Consequently, the cellular concentration of the ferric ion is too low for microorganisms to survive by solely using free iron for survival.

Microorganisms overcome this nutritional limitation in the host by procuring iron either extracellularly from transferrin, lactoferrin, and precipitated ferric hydroxides or intracellularly

from hemoglobin. This is accomplished by microorganisms via two general mechanisms: iron acquisition by cognate receptors using low molecular weight iron chelators termed siderophores and receptor-mediated iron acquisition from host proteins (Fig. 1). The main difference between these two mechanisms is that siderophores and heme can be taken up by the bacterial cell as intact molecules whereas iron must be extracted from host carrier proteins such as transferrin or lactoferrin prior to being transported into the bacterial cell.

The uptake of iron from transferrin, lactoferrin, hemoglobin, and siderophores has been identified in both Gram-negative and Gram-positive bacteria. In Gram-negative bacteria, the outer membrane is a permeability barrier, protecting the bacterium from toxins, degradative enzymes, and detergents. The presence of trimeric β -barrel proteins termed porins in the outer membrane allows for passive diffusion of small solutes that have a molecular weight less than 600 Da [8]. Transferrin, lactoferrin, hemoglobin, and most ferric-siderophore complexes exceed the molecular weight cut off of porins and thus require specific outer membrane receptors for uptake into the periplasmic space. All of these iron uptake pathways involve an outer membrane receptor, a periplasmic binding protein (PBP), and an inner membrane ATP-binding cassette (ABC) transporter. The Gram-negative outer membrane lacks an established ion gradient or ATP to

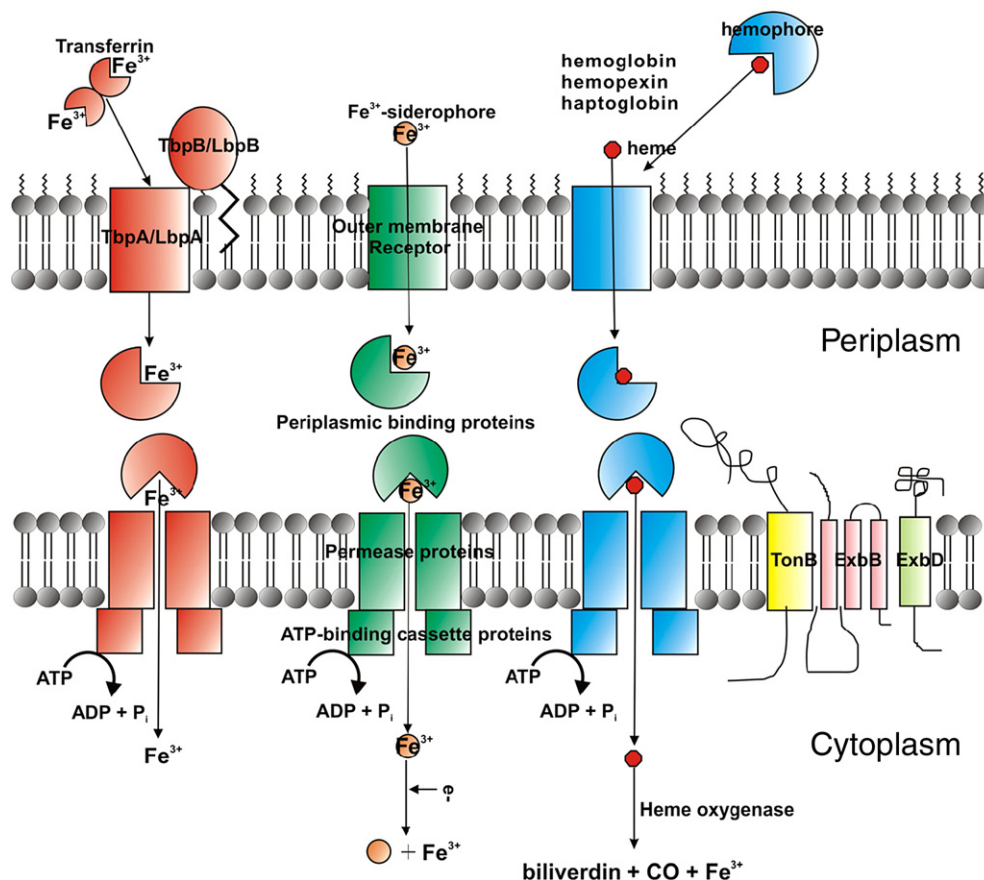


Fig. 1. Schematic representation of iron uptake in Gram-negative bacteria. There are numerous iron uptake pathways in Gram-negative bacteria which include iron uptake from transferrin, siderophores, or heme. All of these uptake pathways require an outer membrane receptor, a PBP, and an inner-membrane ABC transporter. Not all bacteria have all three systems; but some have more than one type. Transport through the outer membrane receptor requires the action of the TonB system (TonB, ExbB, ExbD).

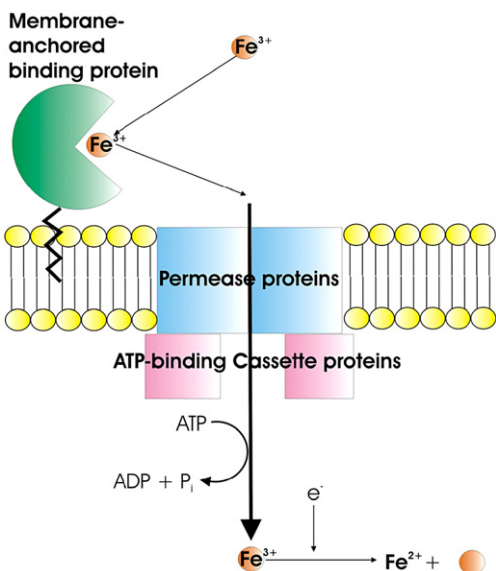


Fig. 2. Schematic representation of iron uptake in Gram-positive bacteria, which unlike Gram-negative bacteria, lack an outer membrane. Therefore, the uptake of iron from heme, siderophore, or transferrin, involves a membrane anchored binding protein and a membrane-associated ABC transporter.

provide the energy for transport. This energy requirement is accomplished through the coupling of the proton motive force of the cytoplasmic membrane to the outer membrane via three proteins: TonB, ExbB, and ExbD. Unlike Gram-negative bacteria, Gram-positive bacteria have no outer membrane. A cell wall composed of murein, polysaccharides, teichoic acids, and cell wall proteins is all that separates the bacterial cytoplasm from its environment. Uptake of an iron source involves a membrane-anchored binding protein, which resembles the PBP in Gram-negative organisms, as well as an ABC transporter (Fig. 2). Recent papers describe the molecular basis of iron uptake in Gram-positive bacteria. However, when compared to Gram-negative bacteria, there is still relatively little information on iron transport in Gram-positive bacteria. The growing availability of genome sequences of Gram-positive bacteria allow for the identification of genes that encode iron transporters that are related to those found in Gram-negative bacteria. This review is limited to a discussion of the structural biology of ferric ion uptake systems. We will focus mostly on Gram-negative bacteria. The iron uptake systems involving transferrin, heme, and siderophores will be briefly described with a more detailed description of available structures of the components of these systems.

2. Transferrin/lactoferrin

Many pathogenic bacteria, such as *Neisseria* and *Haemophilus*, have specific outer membrane receptors that bind to the host's glycoproteins transferrin and lactoferrin [9]. Transferrin and lactoferrin each have a molecular weight of 80 kDa and they are too large to pass through the bacterial outer membrane. Thus, additional steps are required to remove iron from transferrin/lactoferrin at the external surface. Extraction of the iron atoms from transferrin and lactoferrin is thought to occur via the TbpB/TbpA and LbpB/LbpA proteins, respectively. TbpB and LbpB

are 65 to 85 kDa proteins that are attached to the outer membrane with an N-terminal lipid anchor [10]. TbpB, for example, may act as an initial binding site for iron-saturated transferrin, facilitating its subsequent binding to TbpA [11]. TbpA and LbpA are integral membrane proteins that are predicted to have large surface loops that bind to transferrin and lactoferrin, respectively, forcing the separation of the domains surrounding the iron-binding sites to release iron [9–11]. The structures of TbpA/TbpB or LbpA/LbpB have not yet been reported.

Once iron has been transferred into the periplasm, it is bound by the ferric ion binding protein, FbpA, and shuttled to the cytoplasmic membrane where it is transported into the cytoplasm via the FbpB/FbpC cytoplasmic membrane transporters. FbpA is a 37-kDa PBP found in the *Neisseriaceae* and *Pasteurellaceae* families. The structures of iron-free and iron loaded *Haemophilus influenzae* and *Neisseria* sp. FbpA have been determined [12–14] (Fig. 3). More recently, the structures of the FBPs from several other Gram-negative strains have also been determined [15–17]. Although transferrin and FbpA share less than 20% sequence identity, the structure of FbpA has remarkable similarity to the structure of one lobe of transferrin. FbpA has a two-domain structure with two similarly folded lobes consisting of an alternating α -helix/ β -sheet structure connected by two antiparallel β -strands. Comparison of the apo- and holo-FbpA structures of *H. influenzae* reveal a 20°

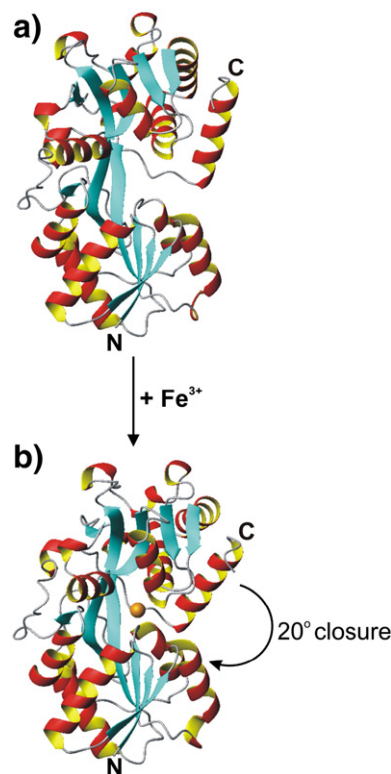


Fig. 3. Ribbon representations of (a) iron-free and (b) iron-bound FBP. *H. influenzae* FBP also demonstrates the “Venus fly trap” mechanism often found in PBPs. Alignment of the N-terminal domains of apo- and holo-FBP reveal a 20° closure upon binding of a ferric ion. The structures of the N- and C-terminal domains remain unchanged regardless whether iron is bound. The individual domains rotate about a hinge created by the central β -strands connecting the two domains.

rotation of the two structural domains about the central β -strands in a “Venus fly trap” domain mechanism (Fig. 3). The Fe^{3+} ion binds in a cleft between the two domains. The Fe^{3+} ion is octahedrally coordinated by two oxygens from Tyr195 and Tyr196, an imidazole nitrogen from His9, a carboxylate oxygen from Glu57, an oxygen atom from an exogenous phosphate, and an oxygen atom from a water molecule [13] (Fig. 4a). In transferrin, the Fe^{3+} is coordinated by similar residues (Tyr92, Tyr192, His253) except that Asp60 replaces Glu and the octahedral coordination is completed with a bidentate (bi)carbonate as the synergistic ion (Fig. 4b). It should be noted that the *Haemophilus* FBP protein contains two adjacent Tyr residues, in its binding site, a feature seen in all bacterial FBPs studied to date (Table 1). In contrast, the two Tyr residues in transferrin are on different domains and they play a role in the closing motion of the iron-binding protein lobes. It was shown by extended X-

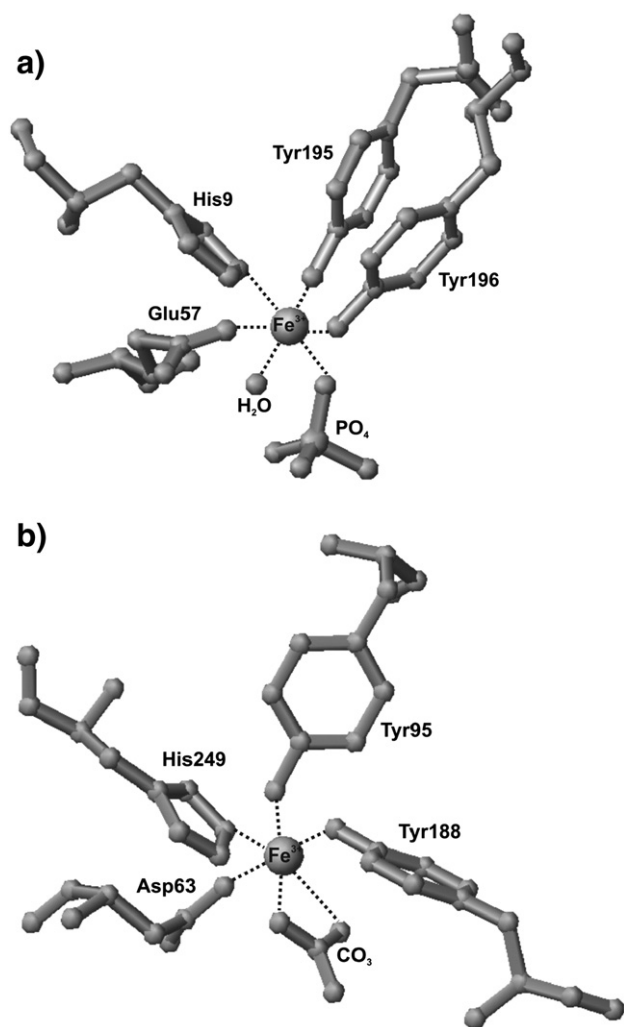


Fig. 4. The Fe^{3+} binding sites of (a) *Neisseria meningitidis* FbpA and (b) the N-lobe of human transferrin. In each protein, the Fe^{3+} ion is coordinated by similar ligands. In FbpA, two oxygens from Tyr195 and Tyr196, an imidazole nitrogen from His9, a carboxylate oxygen from Glu57, an oxygen atom from an exogenous phosphate, and an oxygen atom from a water molecule coordinate Fe^{3+} . In transferrin, the Fe^{3+} is coordinated by similar residues (Tyr92, Tyr192, His253) except that Asp60 replaces Glu and a bidentate (bi)carbonate fulfills the octahedral geometry preferred by Fe^{3+} .

ray absorption fine structure analysis that a carbonate molecule can also act as a synergistic anion for *Neisseria* FbpA, but unlike transferrin, it binds in a monodentate fashion [18]. However, binding of a synergistic anion, while an absolute requirement for binding to transferrins, is not always required for bacterial FBPs, as illustrated by the structure of *Campylobacter jejuni* and *Y. enterocolitica* FBPs [19,20]. Moreover, while Fe^{3+} normally has a strong preference for an octahedral six coordination in two FBP proteins from *Mannheimia haemolytica* and *C. jejuni* only 5 ligands coordinate Fe^{3+} (see Table 1).

3. Heme as an iron source

Under conditions of iron starvation, microorganisms must use all of the iron sources found in their environment. The majority of iron in the body is stored intracellularly in the host proteins ferritin and hemoglobin. The iron component of hemoglobin, heme, can be utilized as a source of essential iron for many microorganisms. Like iron itself heme is cytotoxic and is sequestered by host hemoproteins such as hemopexin. To overcome the limited access to heme, pathogenic bacteria commonly secrete exotoxins such as hemolysins [21–23], cytolytins [24], and proteases [25] that can lyse cells and release the heme bound by host carrier proteins, such as hemoglobins that reside in erythrocytes. For example, the *Escherichia coli* hemoglobin protease (Hbp) was found to be involved in the symbiosis of the pathogenic bacteria *E. coli* and *Bacteroides fragilis* [26]. Hbp is part of the SPATE family (serine proteinase autotransporters of *Enterobacteriaceae*) and it degrades hemoglobin, releasing heme to both bacterial species. Autotransporters consist of the three following parts: an N-terminal signal sequence to target the protein to the periplasm, a passenger domain, and a C-terminal β -domain that forms a β -barrel in the outer membrane, allowing the passenger domain to pass across the outer membrane [27]. The structure of the apo-form of the 110-kDa passenger domain of *E. coli* Hbp is the first complete structure of a passenger domain [28]. The overall structure consists of a long, right-handed β -helical stem (residues 556 to 1048) with two protruding domains. Further studies are required to understand how a heme molecule interacts with Hbp and to determine if Hbp interacts with a surface protein from either *E. coli* or *B. fragilis*.

Microorganisms have two elaborate mechanisms for acquiring heme [29,30]. The first mechanism, the direct uptake of heme or heme associated with host hemoproteins (hemoglobin, hemoglobin-haptoglobin, heme-albumin, heme-hemopexin, and myoglobin), has been identified in both Gram-negative and Gram-positive bacteria [30,31]. In Gram-negative bacteria, heme uptake involves a TonB-dependent outer membrane receptor, a PBP, and an ABC transporter [32]. For example, two receptors that utilize heme as an iron source have been identified in *Neisseria meningitidis*: HpuA/HpuB [33–35] and HmbR [36,37]. HpuA is a 36-kDa lipoprotein and HpuB is an 85-kDa, TonB-dependent, outer membrane receptor. The HpuA/HpuB receptor is a two-component receptor analogous to TbpB/TbpA. It binds hemoglobin, hemoglobin-haptoglobin, and apo-haptoglobin [33,38]. HmbR is an 85-kDa outer membrane

Table 1
Comparison of the coordination spheres of ferric ion-binding proteins from different bacterial species, transferrin, and lactoferrin

Ferric binding protein	Coordinating atoms ^a	Anion ^b	Coordination	Reference
<i>Haemophilus influenzae</i>	Glu ⁵⁷ His ⁹ Tyr ¹⁹⁵ Tyr ¹⁹⁶ H ₂ O	PO ₄ ³⁻ (1)	6	[13]
<i>Neisseria</i> sp.	Glu ⁵⁷ His ⁹ Tyr ¹⁹⁵ Tyr ¹⁹⁶ H ₂ O	PO ₄ ³⁻ (1)	6	[18]
<i>Pasteurella haemolytica</i>	Gln ¹¹ Tyr ¹⁴² Tyr ¹⁹⁸ Tyr ¹⁹⁹	formate	nd ^c	[15]
<i>Mannheimia haemolytica</i>	Tyr ¹⁴² Tyr ¹⁹⁸ Tyr ¹⁹⁹	CO ₃ ²⁻ (2)	5	[16]
<i>Serratia marcescens</i>	His ¹⁴ Glu ⁶² Asp ¹⁴⁴ Tyr ¹⁹⁸ Tyr ¹⁹⁹	Citrate	nd ^c	[20]
<i>Yersinia enterocolitica</i>	His ⁹ Glu ⁵⁷ Tyr ¹⁹⁵ Tyr ¹⁹⁶ H ₂ O	None	6	[17]
<i>Campylobacter jejuni</i>	His ¹⁴ Tyr ¹⁵ Tyr ¹⁴⁶ Tyr ²⁰² Tyr ²⁰³	None	5	[19]
Transferrin	Asp ⁶³ Tyr ⁹⁵ Tyr ¹⁸⁸ His ²⁴⁹	CO ₃ ²⁻ (2)	6	[154]
Lactoferrin	Asp ⁶⁰ Tyr ⁹² Tyr ¹⁹² His ²⁵³	CO ₃ ²⁻ (2)	6	[155]

^a The atoms that coordinate the iron atom are listed with their residue number in superscript.

^b The coordinating anions are either monodentate (1) or bidentate (2) to complete the coordination sphere.

^c The apo structures of these proteins were determined thus their coordination geometries are not yet known.

receptor that shares amino acid similarities with TonB-dependent receptors [37]. Unlike HpuA/HpuB, HmbR is not a two-component system and is specific only to hemoglobin complexes [39].

The heme uptake systems of Gram-positive bacteria consist of a cell surface protein and an ABC transporter [40]. For example, the heme uptake system in *Staphylococcus aureus* consists of the cell surface proteins IsdA, IsdB, and IsdH responsible for the binding of hemopexin-heme, hemoglobin, and haptoglobin-heme, respectively, covalently attached to the cell wall [40,41]. The inner membrane transporter, IsdDEF, transports the heme across the plasma membrane into the bacterial cytoplasm where it is degraded to biliverdin, carbon monoxide, and free iron by the heme monooxygenases IsdG and IsdI [41,42]. With the sequencing of bacterial genomes, similar heme uptake systems have been identified for many pathogenic and non-pathogenic Gram-negative and -positive bacteria [31]. Some structures for the individual components of these heme uptake systems are now becoming available.

For example, structures of the 125-residue heme binding NEAT domains of the *S. aureus* IsdH and IsdA proteins have recently been determined (Fig. 5a) revealing typical β -sandwich structures, with the heme binding pocket lined by several Tyr residues [43,44]. Importantly, a structure from the bacterial ChaN heme transport lipoprotein was recently reported as well [45] (Fig. 5b). While the role of this protein in heme utilization by *C. jejuni* is not entirely clear, it represents a group of some 20 heme binding periplasmic proteins. The protein has a rather asymmetric two-lobe structure, with the smaller domain II which is exclusively α -helical, being responsible for the binding of the heme. Surprisingly in the crystal structure, the protein is dimerized because two heme molecules stack on top of each other; whether this dimerization occurs *in vivo* is presently unclear. Spectroscopic studies reveal that a single Tyr residue plays a role as an axial ligand to the ferric ion, in a similar manner as the heme bound to myoglobin [46] or to the periplasmic ShuT protein from *Shigella dysenteriae* [47]. The latter protein is related to the siderophore-binding proteins discussed later, but binds an intact heme molecule rather than a ferric-siderophore complex.

The second mechanism that bacteria use to extract iron from heme uses specialized bacterial proteins, termed hemophores, which acquire heme from the environment and bring it back to

the bacterial membrane for uptake through a specific transporter. Hemophores have been identified in numerous Gram-negative bacteria [48]. An example of a hemophore system is the heme acquisition system or HAS that has been identified in *Pseudomonas aeruginosa*, *Pseudomonas fluorescens*, *Serratia marcescens*, *Yersinia enterocolitica* and *Yersinia pestis* [49,50]. The hemophore, HasA, is secreted into the bacteria's environ-

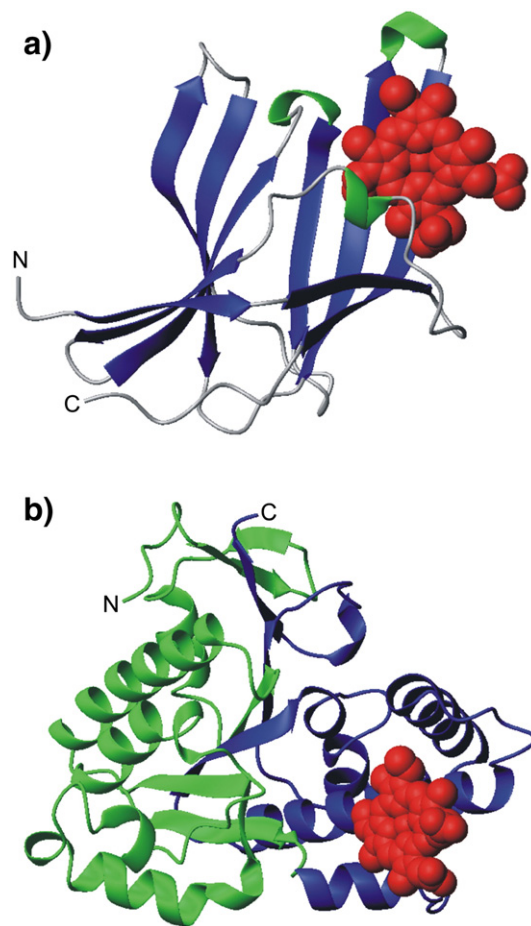


Fig. 5. Ribbon representations of the (a) The NEAT domain of the *S. aureus* IsdA protein colored according to secondary structure and the (b) *C. jejuni* ChaN protein with domains I and II colored green and blue, respectively. The heme molecules are shown in space-filling representation and are colored red.

ment by an ABC transporter composed of a cytoplasmic membrane ABC protein HasD, a second inner membrane protein HasE, and the outer membrane component, HasF [30,48]. Once in the medium, HasA either binds free heme or extracts heme from hemoproteins. The heme bound HasA complex is presented to the outer membrane receptor HasR, which can also recognize a wide variety of substrates including free heme, hemoglobin, hemoglobin–haptoglobin, and heme-albumin. Once the heme has been transported to the cytoplasm it is degraded [51].

The only component of the hemophore-dependent heme acquisition system for which a structure has been determined is the hemophore, HasA, from *Serratia marcescens* [52,53] (N. Wolff, N. Izadi-Pruneyre, J. Couprie, M. Habeck, J. Linge, W. Rieping, C. Wandersman, M. Nilges, M. Dielpierre, A. Lecroisey, unpublished data). The overall structure of HasA is described as a “fish biting the heme” (Fig. 6) [52]. It is a 19-kDa globular protein with a fold showing two faces: a highly curved, 7-stranded antiparallel β -sheet that resembles the letter “s” on one face and four α -helices packed on the other face. The heme-binding pocket is solvent exposed, located between two

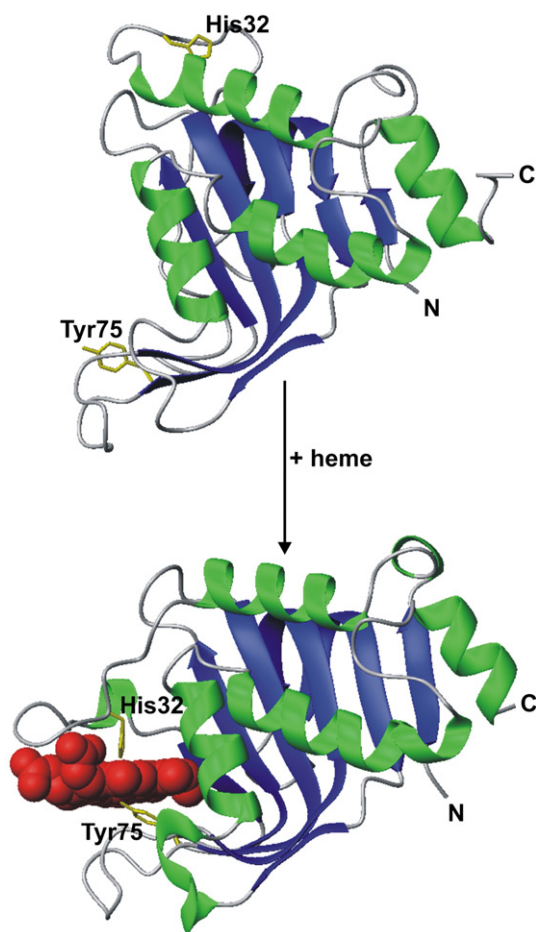


Fig. 6. Ribbon representations of the apo and holo forms of the hemophore HasA from *S. marcescens*. The two residues that ligate the heme molecule (His32 and Tyr75) are shown in stick representation. The heme molecule is colored red and is shown in space-filling representation. The loop containing His32 closes on the heme molecule upon its binding.

loops at the α/β interface of HasA. These loops are composed of a number of hydrophobic residues involved in hydrophobic and stacking interactions with the heme molecule. The N ϵ of His32 and the phenolate of Tyr75 are the axial iron ligands in this pocket (Fig. 6). A third residue, His83, has been shown to stabilize the Tyr75 Fe bond [52–55]. The importance of His32, Tyr75, and His83 residues is apparent with the sequence alignment of HasA from *S. marcescens*, *P. aeruginosa*, *P. fluorescens*, *Erwinia carotovora*, *Y. pestis*. Tyr75 and His83 are conserved between bacterial species. His32 is conserved except for a Gln residue in *Y. pestis*. The two crystal structures obtained at a pH of 4.6 (1B2V) [52] and pH 8.0 (1DKO) [53] show that the O γ of Tyr75 is hydrogen bonded to the N Δ 1 of His83. In contrast, the protein crystal structure obtained at a pH of 6.5 (1DKH) reveals that His83 is in a different orientation and hydrogen bonds with a water molecule, but no longer with Tyr75 [53]. Moreover, the high B-factors and undefined electron density for parts of the heme molecule suggest that the heme molecule is more flexible and that His83 may contribute to heme binding or release. However, this may not be the only structural change involved in heme binding. A structural overlay of the C α backbones of apo-HasA (1YBJ) and holo-HasA (1B2V) shows that no major structural changes occur upon heme binding, with a root mean squared deviation of 1.3 Å, except for the rotation of the loop consisting of residues Gly28 to Gly43 upwards of about 180° upon binding to heme (Fig. 6). This results in His32 moving a total distance of 19.7 Å.

S. marcescens HasA has been further characterized with the determination of a structure of the dimeric form of HasA (DHAsA) [56]. DHAsA is a domain-swapped dimer composed of two HasA molecules and two heme molecules. The overall structure of each monomer of DHAsA is similar to HasA; however, for DHAsA to be identified as a domain swapped dimer, the same structural elements must be swapped between the two monomers. The domains consisting of residues 2–49 are swapped. Although the axial heme ligand, His32, is contained in this swapped domain, the heme binding sites of DHAsA are similar to the monomeric forms of HasA. The only difference is that the heme binding sites of DHAsA are less accessible to solvent due to the domain swapping and the less flexible binding pockets. Dimerization of HasA was shown to not be an artifact of crystallization nor a result of overexpression, but shown to exist in the culture supernatant [56]. Additional studies demonstrating that DHAsA does not deliver its heme molecule to HasR but can transfer a bound heme to a monomer of HasA suggests that DHAsA may have a role as a heme reservoir.

The HasR receptor is part of the TonB-dependent family of outer membrane receptors [57]. Although the structure of the HasR receptor has not yet been determined, sequence alignments, structural alignments, and functional similarities suggest that *S. marcescens* HasR likely has the same cork and barrel organization as the other outer membrane receptors to be described in this review [58]. The model of *S. marcescens* HasR identifies the three following domains: an N-terminal region (residues 1 through 99), a cork domain (residues 100 through 239), and a β -barrel. Heme-bound HasA binds to HasR and the transfer of the heme molecule to HasR is driven through this

protein–protein interaction [59]. The overall structure of HasR and the specific residues involved in interaction between HasA and HasR will be determined with the imminent structure of a HasA–HasR complex [60].

4. Siderophores

Under iron-limited conditions, many Gram-negative and Gram-positive bacteria synthesize low molecular weight iron-chelating compounds known as siderophores. The role of these compounds is to scavenge iron from precipitates or host proteins in the microorganism's extracellular milieu. Currently, there are almost 500 compounds that have been identified as siderophores [61]. Although siderophores differ widely in their overall structure, the chemical natures of the functional groups that coordinate the iron atom are not so diverse. Siderophores incorporate either α -hydroxycarboxylic acid, catechol, or hydroxamic acid moieties into their metal binding sites (Fig. 7) and thus can be classified as either hydroxycarboxylate, catecholate, or hydroxamate type siderophores [62]. Of all of the bacterial iron uptake pathways, the pathway for the uptake of ferric siderophores is the most structurally well defined. The individual components of this uptake pathway will be discussed.

4.1. Outer membrane receptors

Ferric–siderophore complexes exceed the molecular weight cut off of porins and thus require specific outer membrane receptors for their uptake into the periplasmic space. Crystal structures have been determined for the *E. coli* outer membrane hydroxamate, citrate, and enterobactin receptors FhuA, FecA, and FepA, respectively, as well as for the *P. aeruginosa* pyoverdine and pyochelin receptors FpvA and FptA, respectively and the related TonB-dependent vitamin B₁₂ (cobalamin) receptor, BtuB [63–67]. The structures currently available in the protein data bank (PDB) are listed in Table 2 and their structural features are summarized in Tables 3 and 4. Although the sequence identity between each pair of receptors is less than 20%, all of the receptors possess the same following structural components: a 22 antiparallel β -stranded β -barrel and an N-terminal globular domain (which may also be referred to as the cork, plug, or hatch domain) (Fig. 8). The plug or cork domain is located at the N-terminus of each of these receptors and, as its name implies, it occludes the opening of the β -barrel (Fig. 10).

4.1.1. β -barrel domain

The β -barrel domain has the following three main features: 10 short periplasmic loops that range in length from 2 to 10

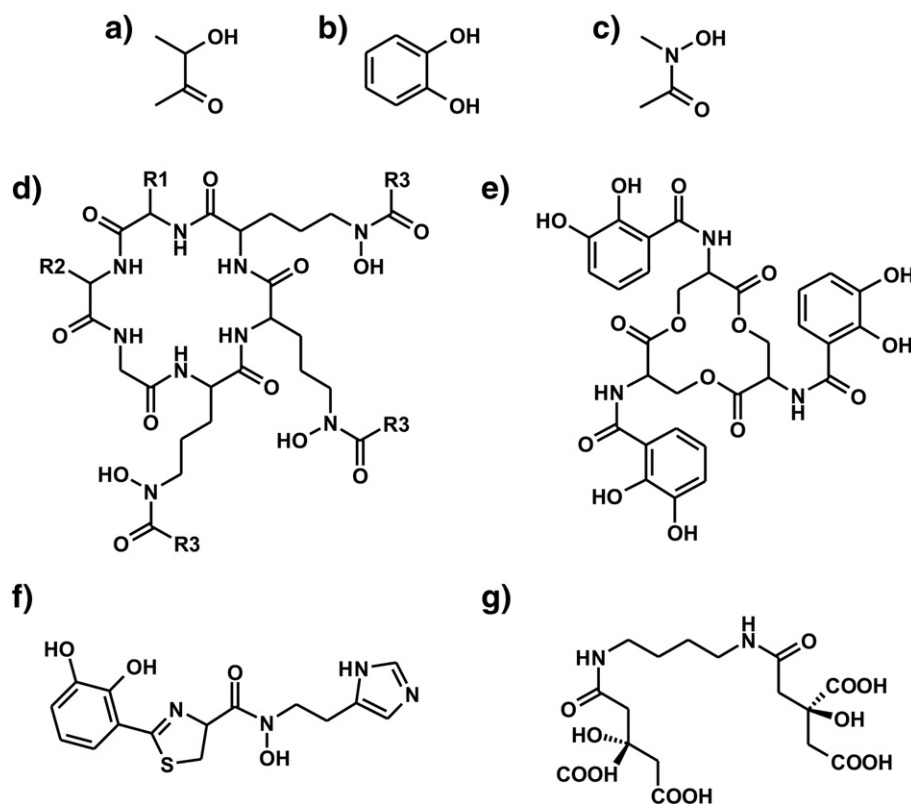


Fig. 7. Functional groups found in siderophores. Although the structures of siderophores may vary, the functional groups for Fe³⁺ coordination are limited. Siderophores usually contain the following metal-chelating functional groups: (a) α -hydroxycarboxylic acid, (b) catechol, or (c) hydroxamic acid. Each functional group is bidentate in that two oxygen atoms are involved in coordinating the iron atom. Since Fe³⁺ prefers a hexa-coordinate octahedral ligand sphere, three of these groups would make up an ideal Fe³⁺ binding site. Since Fe³⁺ is a hard metal ion it also prefers hard ligands, like oxygen. Fe²⁺ is a borderline metal ion that prefers tetrahedral coordination and softer ligands such as nitrogen. Therefore, reduction of Fe³⁺ to Fe²⁺ drastically lowers the affinity of the siderophore for the metal ion and causes its release. A siderophore structure from each chemical class are shown as follows: (d) hydroxamate siderophore ferrichrome, (e) the catecholate siderophore enterobactin, (f) the mixed catecholate-hydroxamate siderophore anguibactin, and (g) the hydroxycarboxylate siderophore rhizoferrin.

Table 2
Currently available structures of *E. coli* and *P. aeruginosa* outer membrane receptors

Outer membrane receptor	Resolution (Å)	PDB code	References
<i>E. coli</i>			
BtuB	2.0	1NQE	[74]
BtuB	2.7	1NQG	[74]
BtuB+Ca ²⁺	3.31	1NQG	[74]
BtuB+Ca ²⁺ +vitamin B ₁₂	3.1	1NQH	[74]
BtuB+colicin E3 receptor	2.75	1UJW	[156]
Cir	2.65	2HDF	[157]
Cir+colicin Ia	2.50	2HDI	[157]
FecA	2.0	1KMO	[66]
FecA+ferric-citrate	2.5	1KMP	[66]
FecA	2.5	1PNZ	[64]
FecA+iron-free dicitrate	2.15	1PO0	[64]
FecA+ferric-citrate	3.4	1PO3	[64]
FepA	2.4	1FEP	[76]
FhuA	2.74	1BY3	[72]
FhuA+ferrichrome	2.6	1BY5	[72]
FhuA	2.5	2FCP	[67]
FhuA+ferrichrome	2.7	1FCP	[67]
FhuA+lipopolysaccharide+rifamycin	2.9	1FI1	[63]
FhuA+ferrichrome	2.7	1QFF	[158]
FhuA+lipopolysaccharide	2.5	1QFG	[158]
FhuA	2.95	1QJQ	[65]
FhuA+albomycin	3.1	1QKC	[65]
<i>P. aeruginosa</i>			
FpvA+pyoverdine	3.6	1XKH	[79]
FptA	2.0	1XKW	[80]

residues, the 22-strand β -barrel, and 11 extracellular loops. Despite limited sequence similarity between the outer membrane transporters BtuB, FecA, FepA, FhuA, FptA, and FpvA, their 22-stranded β -barrels are shown to be structurally similar when the C α backbones of the β -barrels of the outer membrane receptors are overlaid (Fig. 9). Moreover, the angle of the β -strands relative to the axis of the β -barrel is 45° for all of the receptors. The β -barrels are different in their lengths and widths which makes their elliptical shapes vary (Table 3) [68]. The height of the β -barrel varies considerably from 55 Å (BtuB) to 70 Å (FepA). In all cases, the β -barrels extend above the lipid bilayer. The β -barrel is stabilized by inter-strand hydrogen bonds as well as salt bridges connecting strands 1 and 22. Additionally, there is a highly conserved C-terminal Phe (or Trp) residue in all outer membrane receptors that is important for correct folding and insertion in the bacterial outer membrane [69].

Table 3
Dimensions of the outer membrane receptor proteins

Outer membrane receptor	Residues	Cork domain	β -barrel	Dimensions (length, width, height) (Å)
BtuB	594	6–132	137–594	44, 40, 55
FecA	741	80–221	222–741	47, 35, 65
FepA	724	1–153	154–724	40, 30, 70
FhuA	723	1–160	161–723	46, 39, 69
FptA	655	56–186	187–720	45, 40, 60
FpvA	772	129–276	277–815	45, 40, 65

Table 4
Lengths of the extracellular loops for the outer membrane receptors

	Extracellular loops											Total	Average loop length
	L1	L2	L3	L4	L5	L6	L7	L8	L9	L10	L11		
BtuB	3	21	13	12	11	3	18	4	12	20	18	135	12
FecA	9	8	22	2	12	5	18	13	16	24	6	135	12
FepA	7	28	22	21	30	3	37	13	12	25	34	232	21
FhuA	3	6	31	22	26	4	14	7	14	15	23	165	15
FptA	3	5	29	20	22	2	14	21	18	2	23	159	14
FpvA	3	6	32	11	30	4	15	17	13	8	25	164	15

All of the β -barrels have 11 extracellular loops labeled L1 to L11 for all of the transporters. The lengths of these extracellular loops can range from 2 to 37 residues (Table 4) consequently comprising roughly 40% to 50% of the total β -barrel. The extracellular loops can extend 30 to 40 Å above the outer membrane. Their presumed role is to initially interact with the ferric-siderophore as well as occlude the opening of the β -barrel to prevent the access of unwanted solutes.

The structures of FhuA, BtuB, and FecA have been determined with and without their bound ligands ferrichrome, vitamin B₁₂, and ferric-dicitrate, respectively. The ligand-free and ferric-citrate bound FecA β -barrel structures are virtually identical [64]. The only conformational change involves the closing of extracellular loops L7 and L8 towards the ferric-citrate binding pocket. When L7 or L8 is deleted, ferric-citrate is no longer bound or transported thus confirming the importance of the loops [70]. The structure of FecA bound to iron-free citrate does not have the closure of loops L7 and L8 [64]. Thus, it is thought that ferric-citrate replaces the bound citrate molecule. Once ferric-citrate is bound, a conformational change occurs that includes the complete closure of extracellular loops L7 and L8 upon the binding pocket thus preventing the escape of ferric-citrate (Fig. 10). This closure translates into a movement of 11 and 15 Å for L7 and L8, respectively. With the closure of L7 and L8, residues Gln176, Gln570, and Asn721 are able to hydrogen bond with ferric-citrate. This loop closure is not seen in the FhuA crystal structures regardless of the binding of ferrichrome, albomycin, or rifamycin [63,65,67]. However, molecular dynamics simulations suggest that L8 of FhuA closes the binding site upon binding ferrichrome in a similar manner as seen with FecA [71]. The crystal structures of FhuA bound to ferrichrome show that residues from the cork domain (Arg81, Tyr116, and Gly99) and the β -barrel make direct hydrogen bonds or van der Waals contacts with the ferrichrome molecule [67,72]. Tyr244 and Trp246 of L3 and Phe693 of L11 are involved in ferrichrome binding [67]. Deletion of L3 or L11 abolished ferrichrome binding and transport [73]. The deletion of L8 which closed during the molecular dynamics simulations, however, had little effect on ferrichrome transport and increased the level of ferrichrome binding with respect to wild-type FhuA. Thus, the extracellular loops L3 and L11 are important for siderophore binding although it is unknown at present if they close upon ferrichrome binding in a similar manner to L7 and L8 of FecA.

In the structure of ligand-free BtuB, loops L2, L3, and L4 are disordered [74]. L2 and L3 become ordered upon binding of

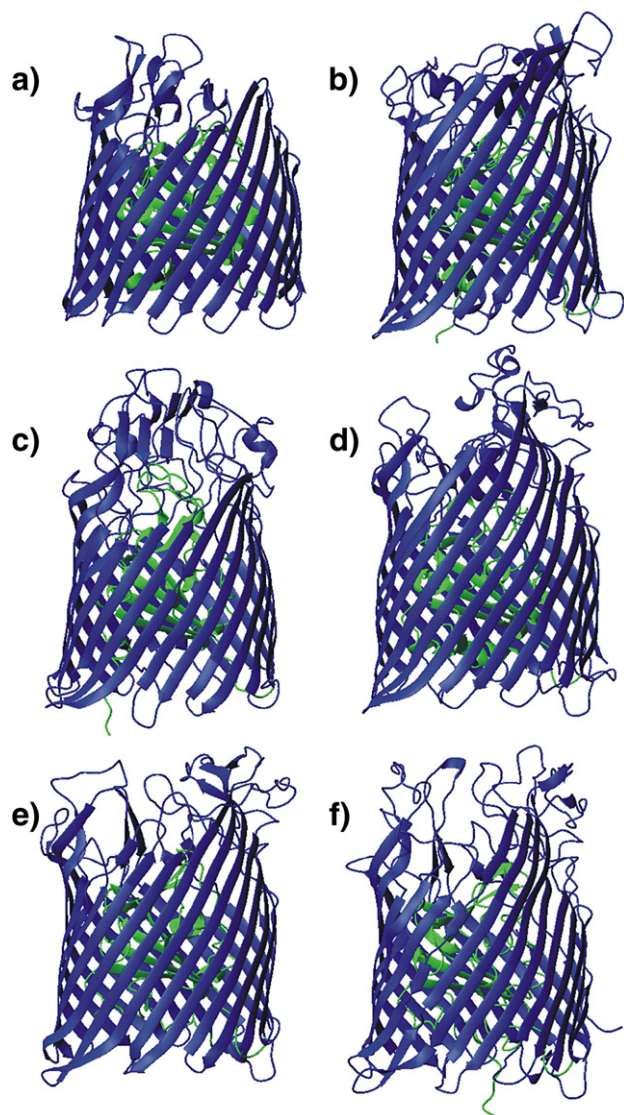


Fig. 8. Outer membrane siderophore receptors from *E. coli* and *P. aeruginosa*. Ribbon representations of the (a) vitamin B₁₂ (BtuB), (b) *E. coli* ferric-citrate (FecA), (c) ferric-enterobactin (FepA), (d) ferric-hydroxamate (FhuA), (e) *P. aeruginosa* pyochelin (FptA), and (f) *P. aeruginosa* pyoverdine (FpvA) receptors. The mixed α - β globular (cork) domain is colored green while the 22-strand β -barrel is colored blue.

Ca²⁺ and all three loops are well defined upon the binding of vitamin B₁₂ [74]. No dramatic loop movement occurs upon vitamin B₁₂ binding. However, because vitamin B₁₂ is a much larger molecule than the ferric-siderophores and the extracellular loops of BtuB are shorter than ferric-siderophore receptors, it may not be possible for the extracellular loops to fold completely over vitamin B₁₂. Deletion studies demonstrated that the loops of BtuB are important. The deletion of L7, L8, L9, and L11 greatly decreased vitamin B₁₂ binding [75]. Although it is possible that FhuA and BtuB have different mechanisms than FecA for binding and transporting their ligands, it is difficult to determine this on the basis of crystal structures alone. Crystal contacts could explain the lack of loop movements. Crystal packing involving the extracellular loops was not only observed for BtuB and FhuA, but also for FepA crystals that were soaked

with ferric-enterobactin [76]. In the latter case, no interpretable density was present to model the bound ferric-enterobactin. This was likely due to the presence of both ferric-enterobactin bound FepA and ligand-free FepA in the unit cell. The formation of crystal contacts through the interaction of the extracellular loops prevented their closure upon the bound ferric-enterobactin thus allowing its escape. Additionally, the crystallization environment is not physiological because of the usually higher ionic strength, the lack of a membrane environment, and the presence of detergents. Lastly, the presence of polyethylene glycols (33% PEG2000 for FhuA and 28–32% PEG1000 for FepA) create osmotic stress. If there is an alteration in the hydration of the protein upon binding of the siderophore, the conformational change may not occur under conditions of osmotic stress. This has been suggested to explain the lack of conformational change observed for the TonB box of BtuB that will be discussed in the following section.

4.1.2. Cork domains

An N-terminal domain (referred to either as the cork, the plug, or the hatch domain) occludes the β -barrel. The structures of the cork domains of FepA, FhuA, FecA, FpvA, FptA, and BtuB all possess a central mixed four-stranded β -sheet with surrounding loops and helices (Fig. 11). The cork domain is kept in place in the β -barrel by 40–70 hydrogen bonds as well as two salt bridges created from four highly conserved residues: two Arg residues in the globular domain and two conserved Glu residues in the β -barrel domain. The features of the cork domain includes apices A, B, and C that are involved with siderophore binding, a TonB box near the N-terminus, and in the case of FecA and FpvA, an N-terminal extension that regulates transcription. Both the extracellular loops and residues located on the apices of the N-terminal cork domain are involved in siderophore binding. The specific interactions with the ligands

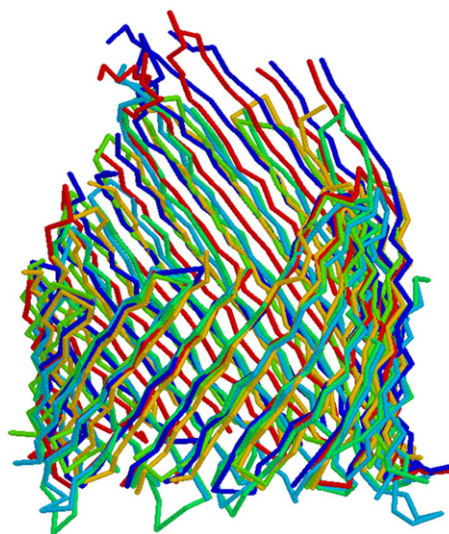


Fig. 9. Superposition of the C_α backbones of BtuB, FpvA, FepA, FecA, and FhuA. Alignment was done using Swisspdb viewer and Molmol. Notice that all the outer membrane receptors have a 22 antiparallel β -stranded barrel. The lengths of the extracellular loops vary between structures and, for clarity, have been removed from the figure.

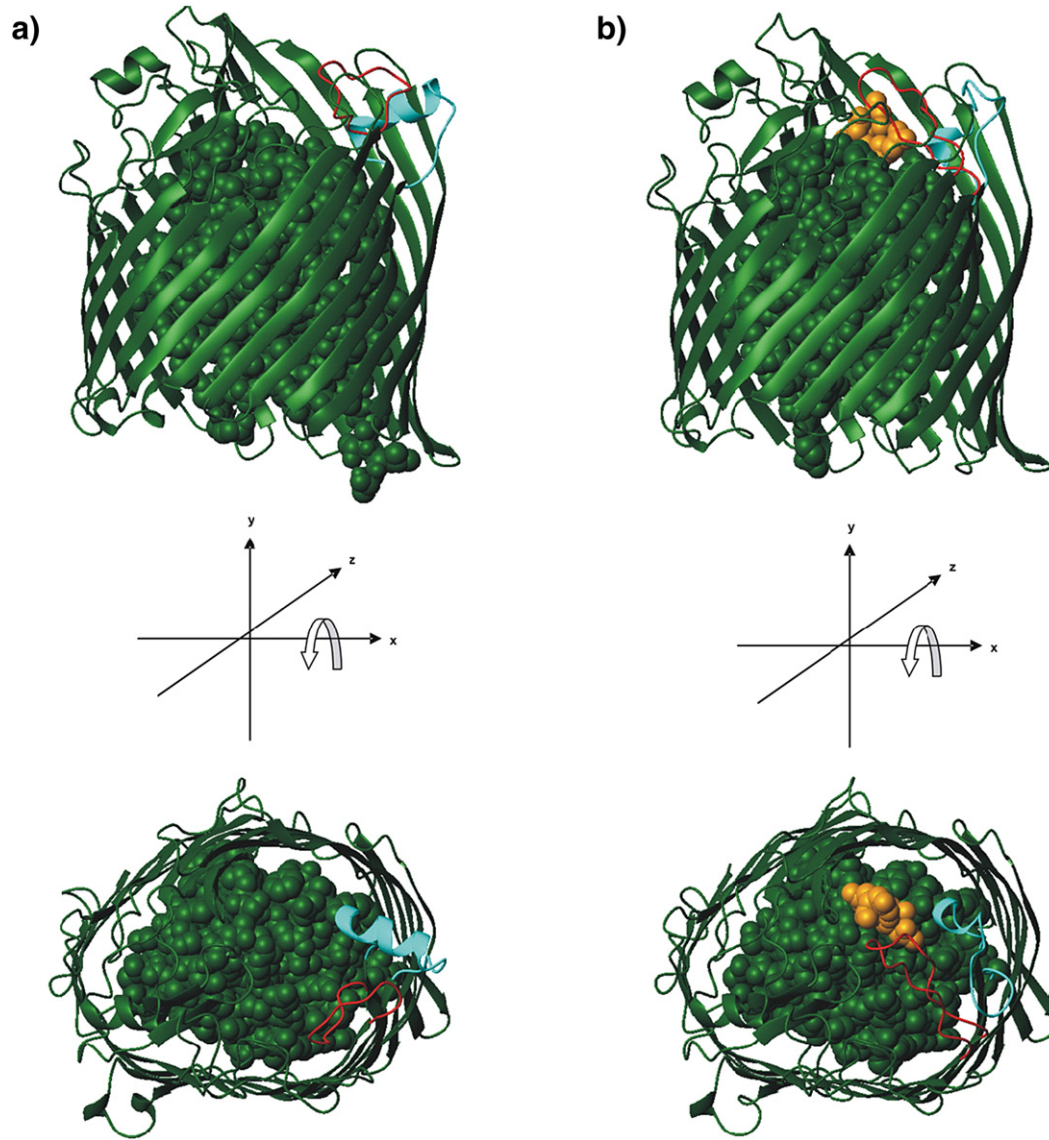


Fig. 10. Ribbon representations of the crystal structures of (a) ligand-free and (b) FecA bound to ferric citrate. The 22- β strand barrel is depicted in ribbon format and the N-terminal cork domain is in space-filling format. The binding of ferric citrate (colored orange) induces a conformational change in the extracellular loops L7 (cyan) and L8 (red) such that the solvent accessibility of ferric citrate is reduced.

and the apices were described for FhuA bound to albomycin [65] or ferrichrome [67], BtuB bound to vitamin B₁₂ [74], and FecA bound to ferric-citrate [64]. Although the apices of the cork domains are involved with ligand binding, they are not the most important component. A study by Scott et al. constructed hybrid proteins of FepA and FhuA in which the cork domain of FepA was replaced with the cork domain of FhuA and vice versa [77]. The empty FepA and FhuA β -barrels selectively bound ferric-enterobactin and ferrichrome, respectively, with wild-type activity. The FepA β -barrel and FhuA cork domain hybrid and the FhuA β -barrel and FepA cork domain hybrid also bound and transported the ferric-enterobactin and ferrichrome, respectively.

The largest changes that accompany ligand binding occur in the N-terminal cork domain. For example, in the structures of FhuA and FhuA bound to ferrichrome, a helix (residues 24 to 29) termed the “switch helix” unwinds when ferrichrome is

bound [63,65,67]. This unwinding changes the position of residues comprising the α -helix with the most dramatic movement involving residue Glu19 which moves close to 17 Å; a significant distance of roughly half the width of the transporter (40 Å). The situation for FecA is different with only partial unwinding of the switch helix (residues 94 to 99) upon siderophore binding [64,66]. The first two residues unwind, but no large displacement of the residues is observed upon ferric-citrate binding. To compare with FhuA, one of the residues that unwinds, Asn95, moves 1.1 Å whereby the second residue of the switch helix of FhuA moves 6 Å. The significance of the switch helix lies in the role of an area of the cork domain termed the TonB box. This is an N-terminal sequence that interacts with the periplasm spanning protein, TonB. This interaction serves to power the siderophore transport through the outer membrane receptor by coupling the proton motive force of the cytoplasmic membrane with the outer membrane. The unwinding of the

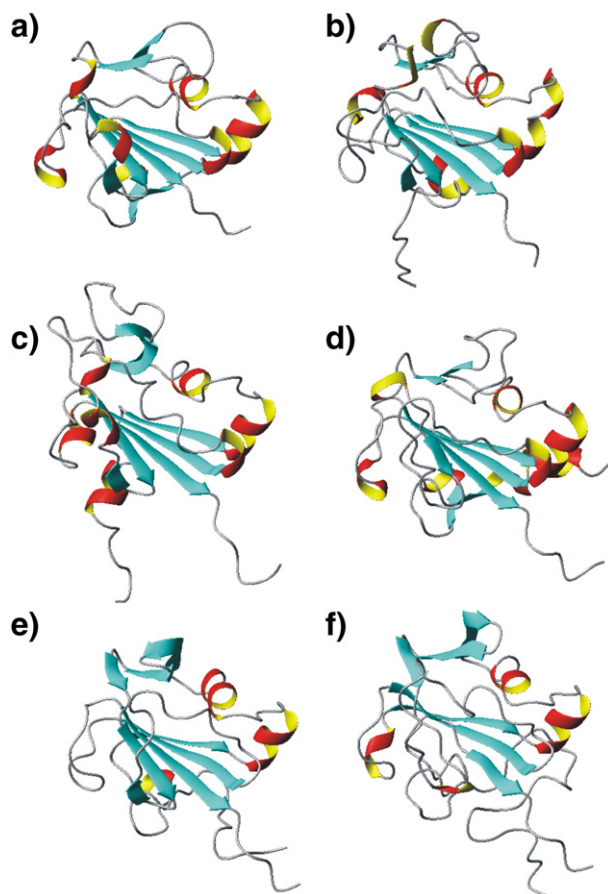


Fig. 11. Ribbon diagrams of the cork domains from the different outer membrane receptors. The cork domains from (a) FecA, (b) FepA, (c) FhuA, (d) BtuB, (e) FpvA, and (f) FptA all show a similar structure with central mixed β -sheet with varying numbers of surrounding α -helices.

switch helix causes a conformational and positional change of the TonB box, resulting in signal transduction to TonB by direct physical contact. The TonB box in the ligand-bound FecA and FhuA structures are disordered and cannot be modeled to the electron density thus indicating their increased mobility upon siderophore binding.

However, in the case of BtuB the TonB box is ordered in both the ligand-free and ligand-bound crystal structures. Spectroscopic techniques demonstrated that this TonB box goes from a folded to an unfolded state upon substrate binding [78]. The spectroscopic techniques also demonstrated that, under osmotic stress similar to the crystallization conditions of BtuB, the conformational change involving the TonB box does not occur. Nonetheless, despite the availability of structures of the ligand-free and bound forms of the outer membrane receptors, it is not evident how the ferric-siderophore travels from the upper binding pocket, past the cork domain, into the periplasm. It is known that energy transfer from the cytoplasmic membrane to the outer membrane receptor promotes ligand internalization. However, it is unknown whether the ligand is transported via the formation of a channel or by the partial or complete displacement of the cork domain. The former is generally the more accepted theory mainly because the energetic barrier that would have to be

overcome by breaking the salt bridges and upwards of 50 hydrogen bonds that occur between the cork domain and the β -barrel [67,76,79,80]. The formation of a transient channel has been confirmed in a study where site-directed disulfide cross-linking tethered the cork domain to the β -barrel of FhuA [81]. The uptake of the ferrichrome analog ferricrocin was similar to that of wild-type FhuA which demonstrated that the complete removal of the cork domain is not necessary for siderophore transport. Detailed analysis of the crystal structures of outer membrane transporters reveals that the interface between the β -barrel and the cork domains are filled with both non-bridging waters (hydrogen bond either to the cork domain or the β -barrel) and bridging waters (hydrogen bond with both the cork and the β -barrel) [82]. This extensive hydration, composed mostly of non-bridging waters, resembles that of a transient protein complex and suggests that the outer membrane protein is favorable to conformational change. Thus, only a modest mechanical force on the cork domain may be sufficient to induce a conformational change. This was demonstrated by steered molecular dynamic simulations of TonB in complex with the Ton box of BtuB where TonB acts as a tether and pulls at the cork domain of BtuB [83]. This pulling results in the partial unfolding of the cork domain, exposing a transient channel that is large enough to allow the substrate to pass through the β -barrel and into the periplasm.

Alternatively, a recent paper demonstrates the removal of the cork domain [84]. Cysteine substitutions were generated for various residues in the loops, β -barrel, and the N-terminal cork domain of FepA. The susceptibility of the cysteine sulfhydryl groups to a fluorophore represented the structural changes that

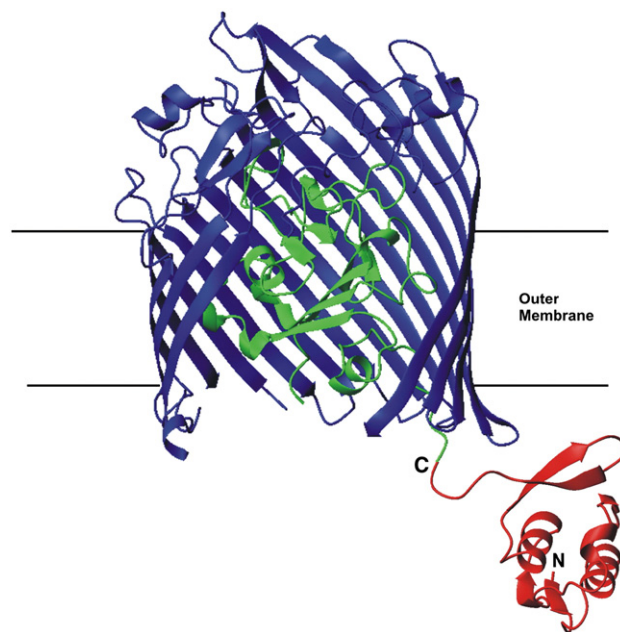


Fig. 12. Ribbon representation of the entire FecA structure. The N-terminal signaling domain (residues 1–79, PDB: 2DIU) is colored red, the β -barrel (residues 81–741, PDB: 1KMO), and the cork domain is colored green (residues 80–221, PDB: 1KMO). For clarity, β -strands from the front section of the β -barrel have been removed. The N- and C-termini of the N-terminal signaling domain (residues 1–79) of *E. coli* FecA are labeled. The position of the FecA N-terminal signaling domain is arbitrary.

occur upon ferric-enterobactin binding and transport. Structural rearrangement of the TonB box was observed by the differential susceptibility of I14C; a residue located on the TonB box. In the absence of ferric-enterobactin, I14C did not react with the fluorophore consistent with the aforementioned folded TonB box. Once ferric-enterobactin was added, the unfolding of the TonB box exposed I14C to the fluorophore. The unexpected reactivity of G54C, a residue located on the N-domain but buried in the interior of the β -barrel, suggests that the fluorophore can access G54 following the removal of the N-terminal domain.

E. coli FecA and *P. aeruginosa* FpvA both have an extra 80 residues located at their N-terminus known as the N-terminal signaling domain. These extra residues are part of a periplasmic signaling domain that is involved in regulation of iron uptake. For example, the *fecABCDE* and *fecIR* system is the most elaborate system found in *E. coli* [85]. FecI is a cytoplasmic σ factor and FecR is a transmembrane anti sigma factor protein consisting of periplasmic, transmembrane and cytoplasmic domains [86]. When ferric-citrate binds to FecA, a conformational change occurring in the N-terminal signaling domain of FecA is transferred to FecR resulting in transmission of a signal across the cytoplasmic membrane that prompts the release of FecI into the bacterial cytoplasm. FecI binds to RNA polymerase which, in turn, binds to the promoter of the *fecABCDE* operon thus initiating the transcription of the ferric-citrate uptake genes. Once *E. coli* has acquired enough iron, Fur-Fe²⁺ binds to the promoter of *fecIR* and *fecABCDE* consequently repressing their transcription. A similar mechanism involving a σ factor (PvdS) regulates pyoverdine synthesis in *P. aeruginosa* [87]. Even though the full-length FecA and FpvA outer membrane receptors have been crystallized [64,66,79], there was no electron density for the N-terminal signaling domain, suggesting that it is either unstructured or flexible. Recently, structures of the 79-residue N-terminal signaling domain plus the adjacent 17 residues of the cork domain (including the TonB box) of FecA (FecA_N) have been reported [88,89]. The overall structure of FecA_N consists of two distinct regions: the structured N-terminal signaling domain (residues 1–79) and the flexible C-terminal tail. The overall structure of the N-terminal region is two adjacent α -helices sandwiched between two short β -sheets (Fig. 12). A similar fold was observed for the periplasmic signaling domain of *P. aeruginosa* FpvA [90]. The flexible C-terminal tail explains why there was no defined electron density for the N-terminal signaling region of FpvA [79] or FecA in either of its bound states [64,66] (Fig. 12).

4.2. Periplasmic siderophore binding proteins

The PBPs are important for escorting their siderophores to the cytoplasmic membrane transporters for subsequent transport into the bacterial cell's cytoplasm. Thousands of hits are obtained upon entering the phrase “periplasmic binding protein” into the NCBI database (www.ncbi.nlm.nih.gov); a number that will undoubtedly grow upon the completion of more bacterial genome sequences. It is necessary to divide this large family into smaller, more manageable classes. An analysis of the amino

acid sequences of PBPs from Gram-negative bacteria and lipoproteins of Gram-positive bacteria revealed a degree of relatedness between the PBPs that allowed for their classification [91]. This analysis produced eight different clusters of PBPs which somewhat correlated with the molecular weight of the protein or the chemical nature of its bound ligand. Proteins that bind oligosaccharides, such as maltodextrin-binding protein (MBP), belong to cluster 1. Proteins that bind organic metal ion complexes include vitamin B₁₂ binding protein (BtuF), and ferric-siderophore complexes (Ceue, FhuD, FepB, FatB, and Rumb), belong to cluster 8. More recently, cluster 9 was introduced [92]. Cluster 9 includes the zinc-binding protein TroA from *Treponema pallidum* [93,94] and the surface manganese-binding protein PsaA from *Streptococcus pneumoniae* [95].

PBPs share a sequence identity often less than 10%. Despite this limited sequence identity, the structures of all of the PBPs which have been solved to date are strikingly similar. PBPs have domains that are connected by either two or three β -strands (clusters 1 to 7) or by a long α -helix (clusters 8 and 9). The fold of each domain is made up of a mixed α/β structure. PBPs that have two domains linked by β -strands move in a “Venus-fly trap” like fashion upon binding and release of their respective ligand much like what was seen for the previously mentioned protein, FBP, which is a member of cluster 1.

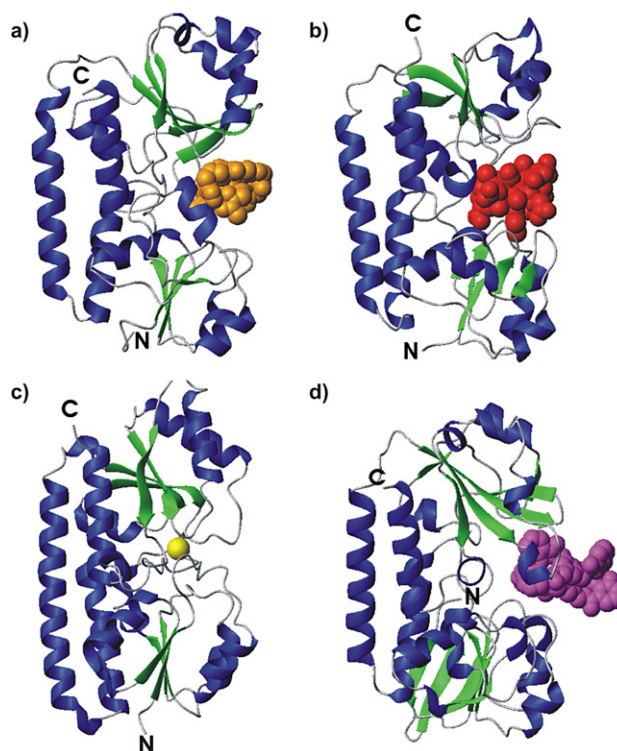


Fig. 13. Ribbon representation of (a) FhuD bound to gallichrome, (b) BtuF bound to vitamin B₁₂, (c) TroA bound to Zn²⁺, and (d) Ceue bound to ferric-mecam. Gallichrome, vitamin B₁₂, Zn²⁺, and ferric-mecam are colored orange, red, yellow, and blue, respectively, and are displayed in space-filling format. Although there is little sequence homology between FhuD, BtuF, TroA, and Ceue, they all have a similar fold consisting of two independently folded domains connected by a long backbone α -helix.

As mentioned in an earlier section, siderophores are classified by their functional groups that coordinate the ferric ion atom as a catecholate, hydroxamate, citrate, or polyhydroxycarboxylate-type siderophore. Because of the chemical distinctness of siderophores, a specific PBP is responsible for shuttling each class of siderophore to the inner membrane. For example, in *E. coli* the PBPs FhuD, FepB, and FecB are responsible for shuttling hydroxamate, catecholate, and citrate-type siderophores, respectively. The siderophore PBPs belong to cluster 8. FhuD is a ferric-hydroxamate binding protein that is found in both Gram-positive and Gram-negative bacteria. It can bind to various hydroxamate siderophores including ferrichrome, coprogen, ferrioxamine B, and rhodoturilic acid. The structures of *E. coli* FhuD bound to gallium-bound ferrichrome (or gallichrome) [96] and various other hydroxamate-type siderophores [97] have all been determined. FhuD is a two-domain protein with the individually folded N-terminal domain (32–145) and the C-terminal domains (169–293) each composed of a twisted five-stranded mixed β -sheet sandwiched between layers of α -helices. The domains are connected by a 23-residue α -helix (residues 145 through 168) that has a kink introduced by the presence of Pro167 (Fig. 13a).

Examination of an overlay of the three dimensional structures of FhuD bound to ferrichrome, albomycin, desferral and coprogen reveals that the binding pockets are similar with only subtle re-arrangement of side chains (Fig. 14). Two highly conserved, key residues are involved in hydrogen bonding with the hydroxamic acid moieties of all of the siderophores: Tyr106 which hydrogen bonds with a carbonyl oxygen and Arg84 which hydrogen bonds with a carbonyl oxygen and/or a nitroxyl oxygen. The chemically different hydroxamate siderophores are accommodated by different hydrogen bonding networks. For instance, additional water-mediated hydrogen bonds occur between residues Gln215 and Ser219 of FhuD and the carbonyl oxygen of the Gly backbone of ferrichrome (Fig. 15a). These water-mediated hydrogen bonds are not found when FhuD is bound to albomycin (Fig. 15b). Unlike the ferrichrome and

albomycin binding sites, the Arg84 sidechain only forms a hydrogen bond with the carbonyl oxygen of Desferral (Fig. 15d). A water-mediated hydrogen bond is observed between Asp61 and a backbone carbonyl oxygen. The coprogen binding pocket varies the most from the other hydroxamate siderophores. There are an increased number of hydrogen bonds between FhuD and coprogen (Fig. 15c). Like the other hydroxamate-type siderophores, Tyr106 hydrogen bonds with the carbonyl oxygen of the hydroxamic acid moiety and the Arg84 sidechain forms only one hydrogen bond with a carbonyl oxygen of coprogen. Tyr275 forms a water-mediated hydrogen bond with a nitroxyl oxygen of the hydroxamate moiety. The coprogen molecule has *trans*-anhydromevalonic acid groups on either end of the hydroxamic acid moieties. To accommodate the insertion of the *trans*-anhydromevalonic acid group into the protein, there is a re-orientation of residue Trp217. With the insertion of this group is the formation of an additional hydrogen bond from Ser103 and a water-mediated hydrogen bond with Trp217 with the hydroxyl group of the *trans*-anhydromevalonic acid group.

FhuD was the only siderophore binding PBP for which a structure had been determined until the structure of the ferric enterobactin binding CeuE of *C. jejuni* was reported [98]. The structure of CeuE in complex with the synthetic catecholate siderophore ferric-mecam demonstrates that the chemical nature of the siderophore defines what composes its binding site. In enterobactin, 2,3-dihydroxybenzoic acid groups are attached to a tris(L-serine) backbone (mesitylene backbone in mecam). When bound to Fe^{3+} , the ferric-enterobactin complex has a net charge of -3 . The ferric-mecam molecules form dimers with a net charge of -6 and each dimer binds to two CeuE molecules. The negatively charged oxygen atoms of ferric-mecam interact with the positively charged Ceu sidechains (Arg117, Arg204, and Arg248). It is apparent that the domain interfaces of PBPs are selective for their ligand. In the case of FhuD, the domain interface is hydrophobic and selective for ferric-hydroxamates whereas the domain interface of CeuE (and likely all the related

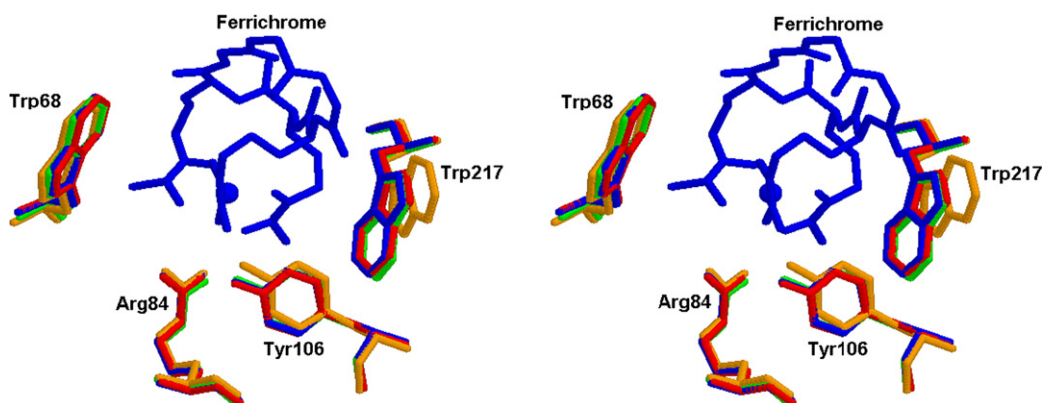


Fig. 14. Overlay of the binding pockets of FhuD bound to ferrichrome (blue), ferric-coprogen (orange), albomycin (red), and desferral (green). The ferric-hydroxamate binding site is composed of hydrophobic residues Trp68 and Trp217 as well as residues Arg84 and Tyr106. The Trp residues interact with the hydrophobic part of the siderophore while residues Arg84 and Tyr106 hydrogen bond with the hydroxamic acid oxygens that are involved with coordinating iron. The binding sites of gallichrome, albomycin, coprogen, and desferral are virtually identical thus demonstrating how FhuD can accommodate various hydroxamate-type siderophores. The only difference is that Trp217 indole ring is rotated in ferric-coprogen bound FhuD. This re-orientation allows for insertion of the *trans*-anhydromevalonic acid group of coprogen into FhuD.

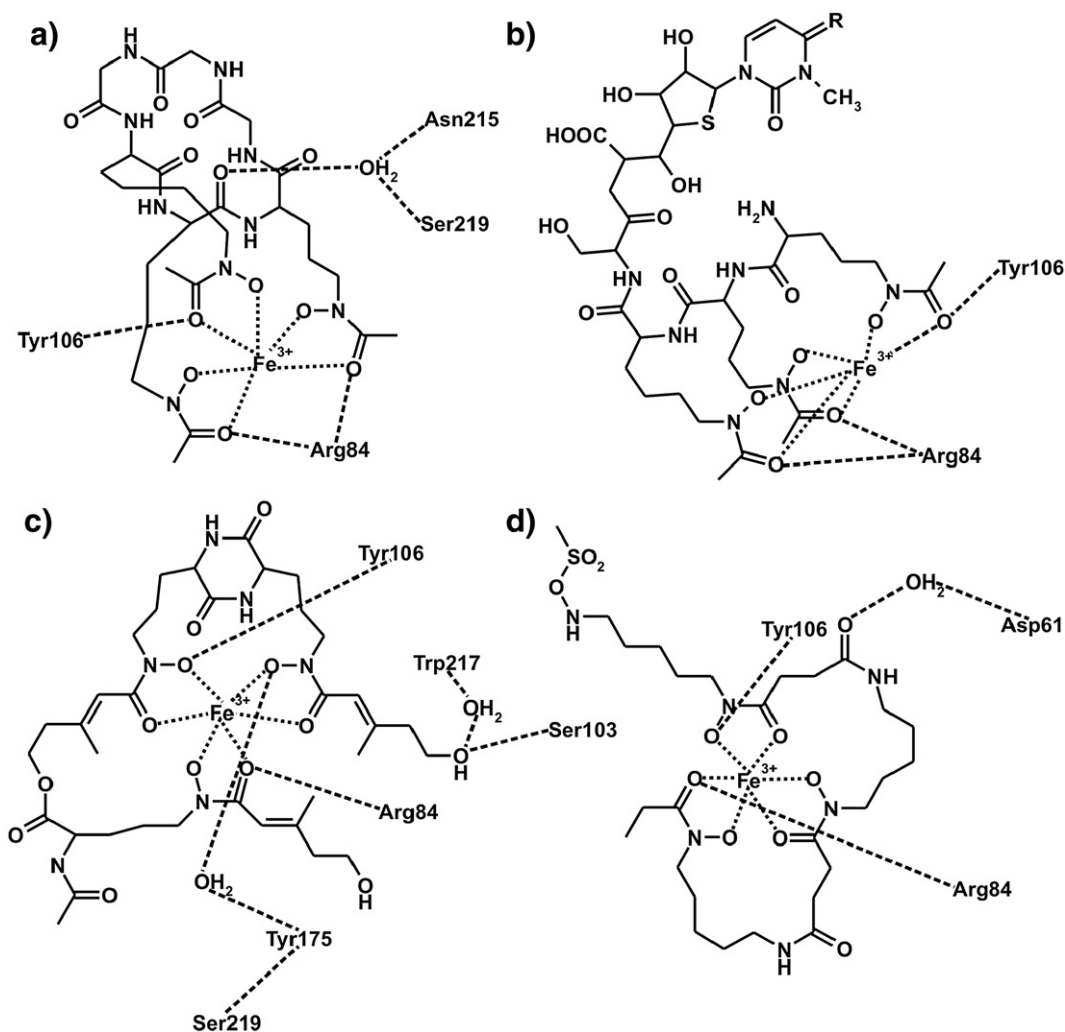


Fig. 15. General structures of hydroxamate-type siderophores and their hydrogen bonding interactions with FhuD. Comparison of binding modes of (a) ferrichrome, (b) albomycin, (c) coprogen, and (d) desferal. The amino acid residues of FhuD and the water molecules that hydrogen bond with each siderophore are labeled with the hydrogen bonds represented as dashed lines.

ferric-enterobactin binding proteins such as FepB from *E. coli* is hydrophilic and selective for ferric-catecholates.

A search using the PDB file of FhuD and the Dali server [99] reveals that the surface manganese binding protein PsaA of *S. pneumoniae* [95], the vitamin B₁₂-binding protein BtuF (Fig. 13b) of *E. coli* [100–102], the zinc-binding protein TroA of *T. pallidum* [93,94] (Fig. 13c), have a similar fold to FhuD and CeuE. The crystallographic structures have been determined for both the bound and unbound forms of FhuD (Krewulak, K.D., Bergmann, E.M., and H.J. Vogel, unpublished results), TroA [93,94] and BtuF [100–102]. Similar to FhuD, both these proteins show no large hinge motion that accompanies the release of their respective ligands [93,94, 100,102]. Like FhuD, BtuF binds a bulky ligand: vitamin B₁₂. When the coordinates of BtuF and FhuD are compared to one another using the Dali server [99], the 262 C α atoms overlaid to give a Z-score of 17.9 and an r.m.s.d. of 3.6 Å. This indicates that even though these two structures share only 17% sequence identity and BtuF is smaller than FhuD

(where the mature forms of FhuD and BtuF are 261 and 244 amino acid residues, respectively), they are structurally very similar.

A least-squares superposition of the N-terminal domains of the bound and apo structures of each BtuF and FhuD (residues 1–106 and 32–145, respectively) show similar degrees of C-terminal domain tilting. The C-terminal domain of BtuF rotates along Pro105 resulting in the C-terminal domain tilting open by 2° about an axis parallel to the backbone α -helix upon release of vitamin B₁₂. Similarly, the C-terminal domain of FhuD appears to rotate about residue Asn146. Here, there also appears to be a 2° rotation about an axis parallel to the backbone α -helix. In both cases, the change of the orientation of the C-terminal domain is not accompanied by an unwinding or bending of the backbone α -helix. This general trend between these two structurally related molecules indicates a similar mechanism for ligand binding and release. The related zinc-binding TroA, unlike BtuF and FhuD, closes somewhat upon release of Zn(II). This is likely related to the more hydrophobic nature of the binding pocket of

FhuD compared to TroA. Since the vitamin B₁₂ and ferrichrome ligands are more bulky than Zn(II), an expansion of the ligand-binding cavity may be essential to facilitate ligand exchange.

Although the X-ray crystallographic structures of cluster 8 and 9 proteins provide some insight into the mechanism of siderophore binding, they do not clearly suggest how the inner membrane transporter, FhuB, distinguishes between ferrichrome-bound and ferrichrome-free FhuD. The α -helix connecting the two domains of FhuD seems to impose rigidity on the structure relative to the β -strands in other “classical” PBPs. Additional rigidity may be imposed on FhuD by the crystal lattice. However, solution small angle scattering studies indicate that the related FhuD2 protein of *S. aureus* undergoes only minimal changes in its overall structure upon binding or release of siderophores [159]. A 30 nanosecond molecular dynamics simulation of FhuD with its bound siderophore removed suggests that individual domains in FhuD may be more dynamic with a C-terminal domain closure of 6° upon release of its siderophore [103]. This relatively large motion suggests structural differences that could allow FhuB to distinguish between apo- and ferrichrome-bound FhuD. In addition, rather extensive molecular dynamics simulations of the apo and holo forms of BtuF suggest that vitamin B₁₂-binding protein may undergo transient opening and closing motions similar to those of the classical PBPs [104]. These intriguing results will need to be verified by future experiments.

5. TonB–ExbB–ExbD

The transport of ferric-siderophores into the periplasmic space requires energy. The proton motive force of the cyto-

plasmic membrane is coupled to the outer membrane via three proteins: TonB, ExbB, and ExbD. ExbB is a 26-kDa cytoplasmic membrane protein. It consists of three transmembrane domains. ExbD is a 17-kDa protein that, like TonB, has only one transmembrane domain and a periplasmic domain of about 90 amino acids. Together, ExbB and ExbD couple the activity of TonB to the proton gradient of the cytoplasmic membrane [105]. The structure of ExbB has yet to be determined. The structure of periplasmic domain of *E. coli* ExbD consists of an N-terminal tail (residues 43–63), a folded region with two α -helices on one side of a 5-stranded β -sheet (residues 64–133), and an unstructured C-terminal tail (residues 134–141) (Fig. 16a) [106]. The structure of the folded region is not unlike the structures of the N- and C-terminal domains of the aforementioned PBPs. A least-squared superposition of the isolated N- and C-terminal domains of FhuD, BtuF, TroA, and CeuE with the folded region of ExbD reveals that ExbD is most like the N-terminal domain of BtuF (residues 1–88) with an r.m.s.d. of 1.5 Å (Fig. 16b). This suggests an evolutionary relationship, however the implications of this structural similarity have yet to be determined.

TonB is a 26-kDa protein that can be considered as a three domain protein. The first domain is an N-terminal domain that consists of the 32-residue transmembrane helix and a short cytoplasmic region. The role of this region extends beyond the anchoring of TonB into the cytoplasmic membrane. TonB interacts with the proteins ExbB and ExbD to form an energy-transducing complex. Replacement of the TonB transmembrane domain with that of TetA, a Gram-negative tetracycline efflux pump that resides in the cytoplasmic membrane [107–109], results in a loss of TonB activity [110]. Additionally, TonB no longer interacts with ExbB suggesting that the interaction of ExbB with TonB must occur between their transmembrane domains.

The central domain of TonB (residues 33–100) is located in the periplasm. Residues 66–102 comprise the characteristic proline-rich region which contains series of Pro–Glu and Pro–Lys repeats. This region may allow for the extension of the protein across the periplasmic space. NMR studies of this isolated region suggest a highly structured conformation that can extend as long as 10 nm [111]. This region does not interact with the outer membrane transporter because deletion of residues 32–65 or 66–100 has no observable effect on the TonB activity [112]. However, when the bacterial cells are exposed to high salt, the periplasmic space expands and the $\Delta(66–100)$ TonB mutant is no longer active, while the wild-type TonB still can function under these conditions. Thus, this region is thought to enhance the efficiency of energy transduction under specific conditions.

The third and final region of TonB is the carboxy-terminal domain (residues 103–239). Various biochemical studies have identified association of this region with the TonB box located in the N-terminal cork domain of the outer membrane receptor. Site-directed disulfide cross-linking studies between the TonB box of BtuB and TonB identify specific residues that interact with one another [113,114]. Additionally, NMR studies using monomeric TonB identified residues that interact with FhuA, FepA, and BtuB derived TonB box peptides using chemical

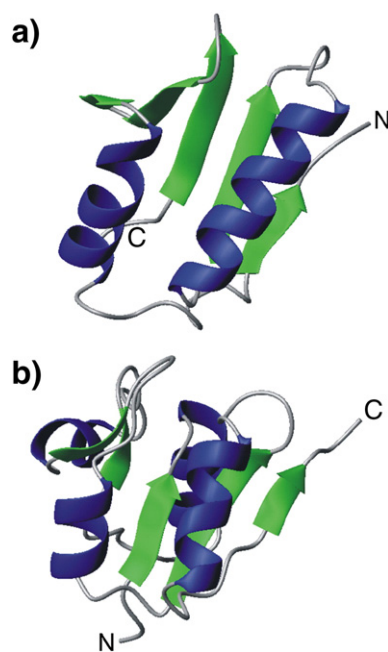


Fig. 16. The structure of (a) ExbD is similar to the N-terminal domain of (b) BtuF (residues 1–88). Both contain a 5-stranded parallel β -sheet. ExbD has two α -helices adjacent to the β -sheet while the β -sheet of the N-terminal domain of BtuF is sandwiched between four α -helices.

shift perturbations [115,116]. More recently, structures of the TonB carboxy-terminal domain in complex with FhuA and BtuB were reported [117,118]. In the structure of the FhuA: TonB complex, creation of an interprotein β -sheet between the Ton-box of FhuA and the central 3-stranded β -sheet of the TonB carboxy-terminal domain was observed. This strand exchange may have functional importance because it positions TonB, allowing the conserved residue Arg-166 of TonB to have an electrostatic interaction with conserved residue Glu-56 of the FhuA cork domain. The structure of the BtuB: TonB complex reveals the formation of a parallel β -strand between the TonB-box of BtuB and the three-stranded β -sheet of TonB. However, the salt bridge of the BtuB: TonB complex is formed between Arg-158 of TonB and Asp-6 of the TonB-box of BtuB, not with the β -barrel as in the FhuA: TonB complex. However, only 5 of the 6 residues of the conserved TonB-box of FhuA were observed in the FhuA: TonB structure. Unambiguous electron density was not observed for Asp-7 of the FhuA TonB-box. Furthermore, the TonB residue Gln-160 previously shown to interact with the TonB-box [119,120] was not observed in the

electron density. It is possible that, similar to the BtuB: TonB structure, Asp-7 of FhuA may have formed a salt bridge with Gln-160 of TonB but, given the lack of electron density, it could not be observed in the FhuA: TonB structure. Not only does TonB contact the outer membrane receptors, but it was recently shown that TonB interacts with the PBP FhuD [121]. Furthermore, when FhuD is added to a FhuA: TonB complex, a ternary complex can be formed. This suggests that TonB could position a PBP near the outer membrane transporter, thereby facilitating the ferric-siderophore to bind to its respective PBP.

The structure of the isolated carboxy-terminal domain of *E. coli* TonB has been solved by X-ray crystallography [122–124] and by NMR spectroscopy [115] (Fig. 17). Most recently, *Vibrio anguillarum* TonB (TonB2) has been solved by NMR spectroscopy (Lopez, C.S., Peacock, S., Crosa, J.H., and H.J. Vogel, unpublished results) (Fig. 17d). The crystal structure of residues 165 to 239 of TonB by Chang et al. is composed of three β -strands and an α -helix. Two monomers of TonB are intertwined with the three β -strands from each monomer combining to form an antiparallel β -sheet. The two more recent structures of a longer fragment of *E. coli* TonB (residues 151–239 for the NMR structure and 150–239 for the X-ray crystallographic structure) and the *V. anguillarum* TonB2 (residues 102–206) do not form an intertwined dimer suggesting that the formation of a dimer in the crystal structure by Chang et al. is likely a result of three-dimensional domain swapping [125] where the exchange of a β -hairpin and C-terminal β -strand between monomers forms the dimer interface [115,123,124]. There are slight differences in the secondary structures of the three *E. coli* TonB structures. For example, when C α backbones of the NMR structure (PDB: 1XX3) and the latest crystal structure (PDB: 1U07) are overlaid, the r.m.s.d. is 0.9 Å. Their secondary structure is identical to one another except for an extra C-terminal β -strand (β 4; residues 235–239) in the NMR structure that folds back to complete the β -sheet. In the crystal structure (PDB: 1U07), the C-terminal β -strand (β 3; residues 220–236) extends away from the TonB structure by eight residues and hydrogen bonds with the β 3 strand of another molecule of TonB to form an antiparallel β -sheet. Although both the NMR and the crystal structures are similar in length, the NMR structure is a monomer while the crystal structure (PDB: 1U07) is a dimer; albeit, not an intertwined dimer like what was observed for the crystal structure by Chang et al. (PDB: 1IHR). Moreover, the small amount of buried surface area in the crystal's dimer interface makes it unlikely that this interaction would be stable *in vivo* [126]. In the structure of *V. anguillarum* TonB2, the C-terminal β -strand (β 4) is absent and the loop joining α 1 and β 3 (loop 3) is extended by 9 Å (Fig. 17d). The β 4 strand plays an integral role in the formation of the dimer interface in TonB structures [122–124]. The lack of β 4 in TonB2 suggests that this protein is unable to form a dimer. The mechanism of the interaction of TonB with the outer membrane receptor is assumed to be universal between bacterial species. Based on this argument, the formation of the TonB dimer likely does not play a major role *in vivo*.

Although TonB appears to exist as a monomer in solution, biochemical data supports both the presence of monomeric and

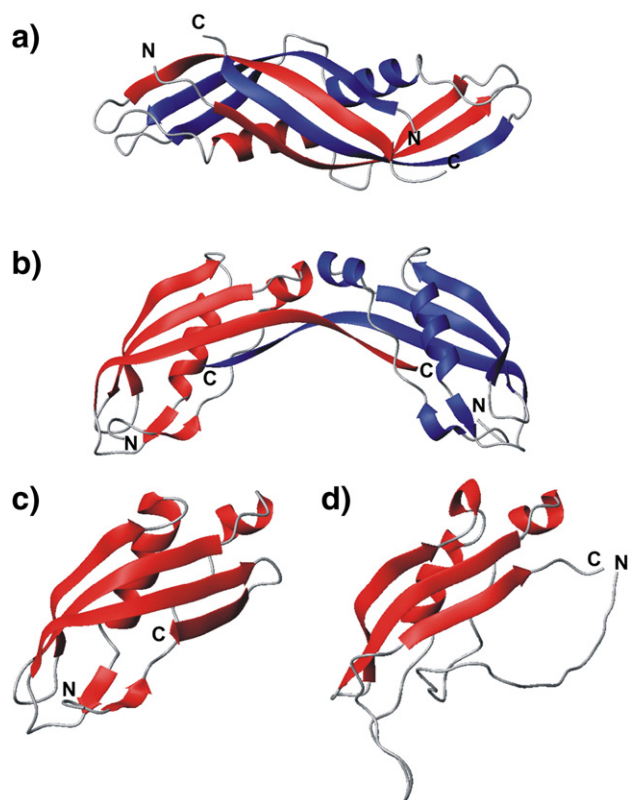


Fig. 17. Structures of the C-terminal domain of TonB. (a) The first crystal structure of TonB (residues 165 to 239) shows two intertwined monomers that may be attributed to domain swapping (Chang et al. 2001). (b) The recent crystal (Koedding et al. 2005) and (c) NMR (Peacock et al. 2005) structures of TonB containing residues 150 to 239 and 151 to 239, respectively. Both have an overall structure of a 4-stranded antiparallel β -sheet in front of two α -helices. The last two structures are quite similar except that the β 4 strand is found at the C-terminal end of the NMR structure, whereas it folds back onto the C-terminal position of a second protein molecule in the recent crystal structure. (d) The recently determined NMR structure of the *V. anguillarum* TonB2, although similar to *E. coli* TonB structures, does not have a β 4 strand and has a significantly longer loop 3.

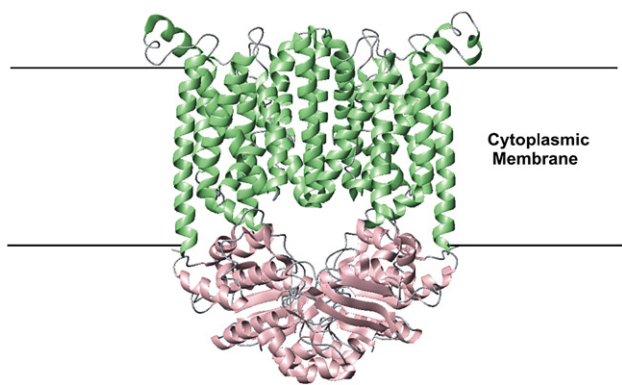


Fig. 18. Ribbon representation of the BtuC₂D₂ ABC transporter of *E. coli*. BtuCD is a tetrameric protein comprised of two α -helical transmembrane subunits (green) and two cytoplasmic ABC proteins (pink).

dimeric forms of TonB. TonB dimerization was studied *in vivo* by constructing hybrid proteins from TonB (residues 1 to 239, 22 to 239, or 164 to 239) and the transcriptional activator of the cholera toxin gene, *ctx*, ToxR [127]. When ToxR dimerizes, *lacZ*, under the control of the *ctx* promoter, is transcribed. It was shown that TonB(164–239) had the greatest propensity to form dimers. Similarly, an ultracentrifugation study on various lengths of the TonB carboxy-terminal domain demonstrated that the smaller fragments of TonB form dimers whereas the larger fragments exist as monomers in solution [123]. Moreover, a shorter, dimer-forming fragment of TonB (TonB-77) was unable to bind FhuA *in vitro* and is resistant to bacteriophage Φ 80 infection *in vivo* wherein the monomeric forms of TonB interact with FhuA and are susceptible to bacteriophage Φ 80 infection. Therefore, dimerization of TonB does not appear to facilitate its binding to the outer membrane receptor, FhuA. An earlier study identified an aromatic cluster of five residues in the carboxy-terminal 75 amino acids of TonB (Phe180, Phe202, Trp213, Tyr215, and Phe230) that, when mutated to Ala, affected TonB function [128]. In an *in vivo* study of full-length TonB each of these five aromatic amino acids were mutated to Cys [129]. Four out of five of these aromatic residues (Phe180 the exception) could interact with one another to form disulfide-linked dimers *in vivo* [129]. Furthermore, the formation of these dimers required the full-length TonB protein and the proton motive force (provided by ExbB/ExbD and TolQ/TolR). None of the currently available structures for TonB are consistent with this *in vivo* biochemical data suggesting that TonB may exist in an energized conformation not yet identified *in vitro*. This can be explained with one of the current model for TonB energy induction [130]. First, the TonB, ExbB, and ExbD proteins form a complex. Quantification of the TonB, ExbB, and ExbD reveals that their ratio in the cell is 1 TonB:2 ExbD:7ExbB [131], although this does not necessarily reflect the stoichiometry of the complex in the cell. ExbB and ExbD harvest the cytoplasmic membrane proton motive force, transmitting it to the transmembrane domain of TonB, energizing TonB. The formation of the previously discussed aromatic cluster may occur at this step. This is supported by the presence of disulphide linked dimers only in the cytoplasmic membrane fractions [129]. The third step occurs when TonB spans the periplasmic space and associated

with the TonB box of the ligand-bound outer membrane receptor. TonB releases its conformationally stored potential energy which results in the active transport of the ligand into the periplasmic space. Thus it is still possible that a monomer/dimer equilibrium plays a role in the energy transduction mechanism.

6. ATP-binding cassette transporters

Once the siderophore has been bound by a PBP, it must be transported into the cytoplasm. This is accomplished by an ABC transporter protein complex which couples ATP hydrolysis to the transport of the siderophores. Bacterial ABC transporters commonly consist of four structural domains: two transmembrane domains that form a channel where the ferric-siderophore passes through and two nucleotide binding domains that hydrolyze ATP. Bacterial ABC transporters are usually assembled from separate subunits rather than fused into one signal polypeptide. Such is the case for the vitamin B₁₂ importer from *E. coli* (BtuC₂D₂), the ferric-enterobactin importer from *E. coli* (FepC₂D₂), and the ferric-enterobactin importer from *V. anguillarum* (FatC₂D₂). In contrast, the hydroxamate siderophore importer from *E. coli*, FhuBC, has the FhuB dimer fused into one polypeptide chain, but like the other ATP-binding domains, two copies of FhuC assemble to form a dimer (FhuBC₂).

The diversity of transported substrates is reflected in the roughly 25% sequence identity between different membrane-spanning domains BtuC, FhuB, FepD, and FatC. The outer membrane receptor (BtuB) and the periplasmic protein, BtuF, are structurally similar to those of the siderophore uptake mechanism of bacteria. A sequence alignment of the ABC transporter, BtuC₂D₂ with FhuBC₂, FecC₂D₂, and FepC₂D₂ reveals sequence identities/similarities of 26%/40%, 35%/53% and 25%/45%, respectively. Thus the structure determined for BtuC₂D₂ is a good representative for FhuBC₂, FecC₂D₂, and FepC₂D₂ and hence will be discussed in detail [132].

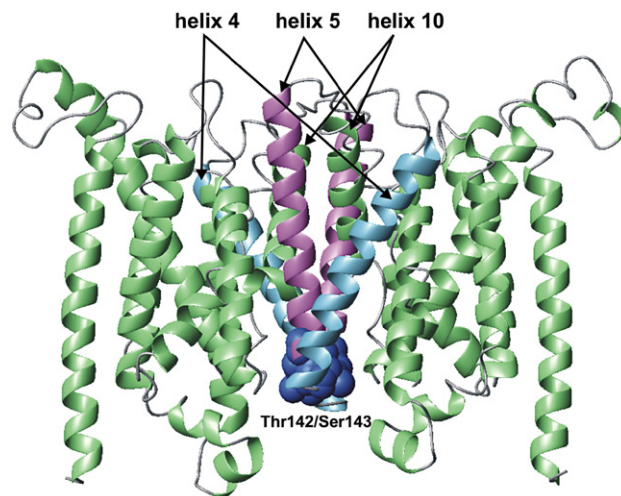


Fig. 19. Ribbon representation of the BtuC dimer. The pathway for vitamin B₁₂ is open to the periplasm but closed to the cytoplasm by a gate region. The gate region occurs between residues Thr142 and Ser143 (in space filling format and colored dark blue) that are located in the loop region between helix 4 (light blue) and helix 5 (violet) of each BtuC monomer.

The overall structure of BtuC₂D₂ contains 10 transmembrane helices per BtuC subunit (Fig. 18). At the interface between the two BtuC subunits, there is a large cavity that opens up to the periplasmic space, but there is not a complete channel visible

across the membrane. The cavity is formed by four helices: helices 5 and 10 from each BtuC subunit and are lined by hydrophobic residues. It is large enough to accommodate a molecule of vitamin B₁₂, but it does not have the same residues

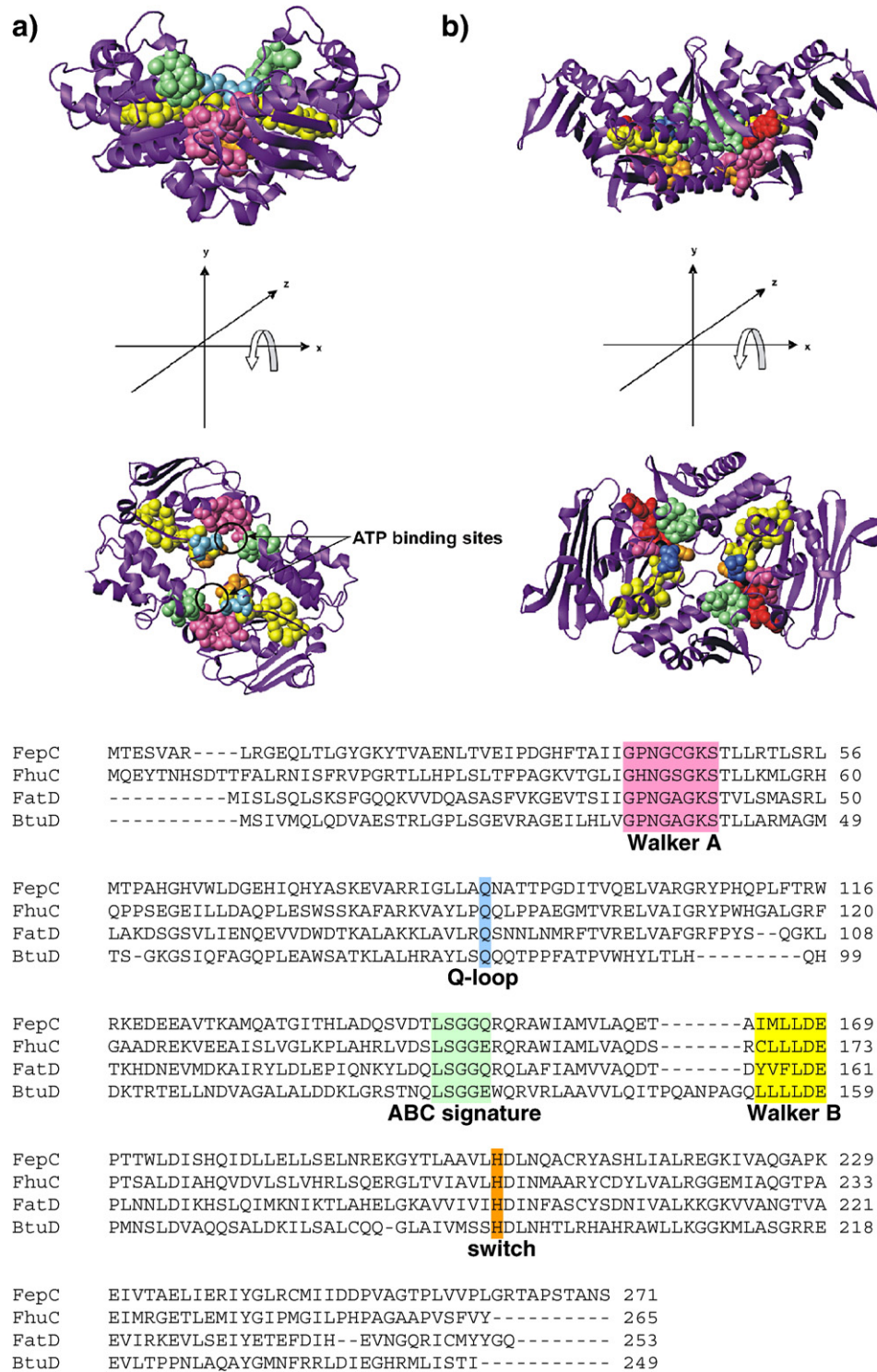


Fig. 20. Space filling representation and sequence alignment of the conserved motifs of ABC subunits. The P-loop/Walker A (pink), Q-loop (blue), ABC-signature (green), Walker B (yellow), and switch loop (orange) motifs are colored accordingly between the sequence alignment and (a) BtuD₂ and (b) Rad50 bound to ATP. ATP is bound at the dimer surface between a Walker A motif (pink) of one monomer and the ABC signature motif (green) of the opposing monomer. The ATP molecules and their bound Mg²⁺ atoms are colored red and black, respectively. The site in BtuD where ATP would bind is circled.

as the vitamin B₁₂ binding site of BtuF thus suggesting its role as a transport channel and not a binding site [100,102]. Residues Thr142 and Ser143 form a gate region in the loop between helix 4 and helix 5 of the two membrane spanning BtuC subunit (Fig. 19) thus closing off the cavity from the cytoplasm.

Structures have been reported for the ATP-binding proteins *E. coli* HisP [133], *Thermococcus litoralis* and *E. coli* MalK [134,135], human TAP1 [136], *Methanococcus jannashii* MJ1267 [137], *M. jannashii* MJ0796 [138], *Pyrococcus furiosus* Rad50 [139], the multisugar transporter from *Sulfolobus solfataricus* GlcV [140], *E. coli* HylB [141], and human CFTR [142]. Despite the large diversity of substrates, ATP-binding domains share conserved sequence motifs that are vital for ATP binding and hydrolysis. These highly conserved motifs include the Walker A motif (GxxGxGKS/T where x can be any amino acid), the Walker B motif (hhhhD where h is a hydrophobic amino acid), the “signature sequence” that is unique to the ABC transporter family (LSGGQQ/R/KQR), the switch region that contains a His residue, and the Q-loop that has a conserved Gln [143]. Similarly, a sequence alignment of FhuC, FepC, FatD with BtuD demonstrates the conservation of these sequence motifs (Fig. 20).

Formation of a dimer between two ATPase units is necessary for an ATP molecule to bind because ATP interacts with the Walker A motif of one monomer and the signature sequence of the other monomer (Fig. 20). The Walker A motif usually forms a loop that wraps around the negatively charged phosphates of ATP and ADP. It is yet unknown what the signature motif's function is although it has been suggested to be a γ -phosphate sensor. Mutation of the Ser residue in the signature motif in Rad50 (S793R) results in the loss of ATP-dependent dimerization [139]. The signature motif is often found mutated in the CFTR (cystic fibrosis transmembrane conductance regulator) of cystic fibrosis patients (the S549R mutant is the most common) [144,145]. The Gln residue of the Q-loop coordinates the Mg²⁺ atom that is coordinated by ATP either directly as in the Rad50 structure or indirectly as was found in the TAP1 structure. The Walker B motif forms a β -strand. The Glu residues either coordinate the Mg²⁺ or polarize a water molecule that attacks the γ -phosphate of ATP. A Gln residue located in the “Q-loop” also coordinates the Mg²⁺. The His residue in the switch region is thought to either sense that a γ -phosphate has bound or it polarizes a water molecule that will assist in the hydrolysis of ATP. Thus, it is assumed that all ABC proteins bind and hydrolyze ATP in a similar way.

The available structures of ABC transporters have allowed for some speculation of substrate transport. Alignment of the structure of BtuF with BtuCD reveals that conserved glutamates on the apices of the lobes of BtuF are adjacent to the conserved Arg residues of BtuCD [100]. Thus it had been suggested that the formation of salt bridges allows for the docking of BtuF onto BtuCD (Fig. 21). Similar electrostatic interactions have been observed in the structure of the molybdate binding protein ModA in complex with its ABC transporter ModB₂C₂ [146]. Numerous charged amino acid residues on the surface of ModA contribute to the ModA–ModB₂ interface. In the ABC transporters, the nucleotide binding site and substrate channel are

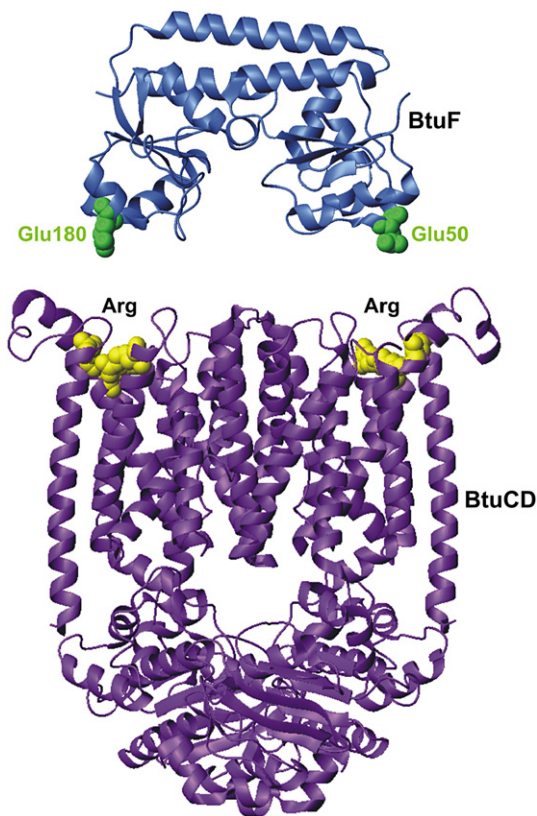


Fig. 21. Proposed docking interaction of BtuF with its ABC transport, BtuC₂D₂. The negatively charged Glu residues (colored green, shown in space-filling format, and numbered according to the PDB file 1N4A) located on the apex of each lobe of BtuF could potentially interact with the positively charged Arg residues (color yellow and shown in space-filling format) located in the periplasmic-facing pockets of BtuC. The formation of salt-bridges would induce a conformational change that would then allow for the transport of vitamin B₁₂ through BtuC and into the cytoplasm.

separated by a membrane. To prevent the hydrolysis of ATP in the absence of bound PBP, there must be a signal to the ATPase component to indicate that the PBP has bound. This communication is thought to occur through the interface region; i.e. where the transmembrane domains and ATPase interact. The BtuF–BtuC₂D₂ complex can be formed in the absence of ATP [100]. Conversely, the formation MalE–MalFGK₂ required ATP and vanadate [147]. Vanadate acts as an analog of the γ -phosphate of ATP. It forms a complex with magnesium and ADP that mimics the transition state of ATP during hydrolysis [148,149]. In the same study the authors found that the maltose binding protein (MalE) docked onto MalFGK₂ no longer had bound maltose when, previously, it had been found to be difficult to obtain MalE free of bound maltose [150]. This indicates that the transport of maltose has already occurred and MalE still remains bound to MalFGK₂. Regardless of the substrate, the transport process is powered by ATP hydrolysis. When BtuF docks onto BtuC₂, there must be some conformational change that occurs. First, BtuF binds followed by a conformational change that is transmitted to BtuD₂ [151]. ATP binds and BtuF has a reduced affinity for vitamin B₁₂ thus releasing it to the channel. The transporter is thought to be in an inward-facing state such as was seen in the structure of

ModB₂C₂A [146] and the recently determined HI1470/71 [152]. Once ATP hydrolysis occurs, a conformational change closes the gap between the conserved ATP-binding motifs. Subsequently, the transmembrane domains flip to an outward-facing conformation [132,153] and vitamin B₁₂ is transported into the cytoplasm. ADP and P_i is released and BtuC₂D₂ is reset to its original conformation.

7. Conclusions

The structural biology of the components of the iron uptake system in Gram-negative bacteria has provided an overall view of the mechanisms of iron transport, but also raises many more questions. First, the presence of a cork domain occluding a β -barrel was unique when compared to the structures of previously determined outer membrane transporters. However, it is still not understood how the ferric-ligand can be transported into the periplasm—is the cork completely removed from the barrel or is a transient channel formed? Second, numerous biochemical experiments confirm that the C-terminal domain of TonB interacts with the TonB box of the outer membrane receptors. This interaction can be seen in the structure of TonB with the outer membrane proteins FhuA and BtuB [117,118]. Additional questions regarding TonB include whether TonB exists in different energized forms and, if ever, does TonB play a role as a dimer *in vivo*. Several more biochemical experiments as well as a structure of the full-length TonB alone and in complex with ExbB and ExbD are required for a comprehensive molecular image of TonB/ExbB/ExbD. Third, clusters 8 and 9 of the PBPs are fairly new. The N- and C-terminal domains of FhuD, BtuF, TroA, and CeuE are connected by a single α -helix rather than two or three β -strands commonly found in other PBP thus restricting any large domain motion upon binding a siderophore. With such a small domain motion, how can the inner membrane ABC transport distinguish between the apo and holo forms of these proteins? Extensive studies using solution NMR as well as small angle X-ray scattering should be completed using several representatives from the PBP clusters 8 and 9 to further understand the range of motions that are open to this group of proteins. Fourth, it has been hypothesized how a PBP interacts with its ABC transporter for subsequent transport of the ligand into the cytoplasm; however, there is little experimental evidence to support this. Although there is a crystal structure of the ModA protein in complex with its ABC transporter ModB₂C₂ [146], neither structure resembles the PBPs or ABC transporters that govern bacterial iron uptake. Ultimately, a crystal structure of BtuF docked onto its ABC transporter BtuCD would give more insight.

Note added in proof

While this paper was being typeset, a paper showing this complex appeared [160]. Although the mechanisms and the structures of the individual components of iron uptake in Gram-negative bacteria have begun to be understood, there is obviously still a lot that needs to be learned.

Acknowledgements

Research on bacterial iron uptake is supported by an operating grant from the Canadian Institute for Health Research (CIHR). K.D.K. was the holder of postgraduate awards from the Natural Sciences and Engineering Research Council of Canada (NSERC) and Alberta Heritage Foundation for Medical Research (AHFMR). H.J.V. holds a Medical Scientist Award from the Alberta Heritage Foundation for Medical Research (AHFMR).

References

- [1] E.D. Weinberg, The Lactobacillus anomaly: total iron abstinence, *Perspect. Biol. Med.* 40 (1997) 578–583.
- [2] F. Archibald, *Lactobacillus plantarum*, an organism not requiring iron, *FEMS Microbiol. Lett.* 19 (1983) 29–32.
- [3] B. Bruyneel, M. Vande Woestyne, W. Verstraete, Lactic acid bacteria: micro-organisms able to grow in the absence of available iron and copper, *Biotechnol. Lett.* 11 (1989) 401–406.
- [4] M. Imbert, R. Blondeau, On the iron requirement of lactobacilli grown in chemically defined medium, *Curr. Microbiol.* 37 (1998) 64–66.
- [5] D. Pandey, F. Bringel, J.-M. Meyer, Iron requirement and search for siderophores in lactic acid bacteria, *Appl. Microbiol. Biotechnol.* 40 (2005) 735–739.
- [6] D. Touati, Iron and oxidative stress in bacteria, *Arch. Biochem. Biophys.* 373 (2000) 1–6.
- [7] B. Halliwell, J.M. Gutteridge, Oxygen toxicity, oxygen radicals, transition metals and disease, *Biochem. J.* 219 (1984) 1–14.
- [8] H. Nikaido, Molecular basis of bacterial outer membrane permeability revisited, *Microbiol. Mol. Biol. Rev.* 67 (2003) 593–656.
- [9] S.D. Gray-Owen, A.B. Schryvers, Bacterial transferrin and lactoferrin receptors, *Trends Microbiol.* 4 (1996) 185–191.
- [10] A.B. Schryvers, I. Stojiljkovic, Iron acquisition systems in the pathogenic *Neisseria*, *Mol. Microbiol.* 32 (1999) 1117–1123.
- [11] I.C. Boulton, A.R. Gorrings, J.K. Shergill, C.L. Joannou, R.W. Evans, A dynamic model of the meningococcal transferrin receptor, *J. Theor. Biol.* 198 (1999) 497–505.
- [12] C.M. Bruns, D.S. Anderson, K.G. Vaughan, P.A. Williams, A.J. Nowalk, D.E. Mcree, T.A. Mietzner, Crystallographic and biochemical analyses of the metal-free *Haemophilus influenzae* Fe³⁺-binding protein, *Biochemistry* 40 (2001) 15631–15637.
- [13] C.M. Bruns, A.J. Nowalk, A.S. Arvai, M.A. McTigue, K.G. Vaughan, T.A. Mietzner, D.E. Mcree, Structure of *Haemophilus influenzae* Fe³⁺-binding protein reveals convergent evolution within a superfamily, *Nat. Struct. Biol.* 4 (1997) 919–924.
- [14] S.R. Shouldice, D.R. Dougan, R.J. Skene, L.W. Tari, D.E. Mcree, R.H. Yu, A.B. Schryvers, High resolution structure of an alternate form of the ferric ion binding protein from *Haemophilus influenzae*, *J. Biol. Chem.* 278 (2003) 11513–11519.
- [15] S.R. Shouldice, D.R. Dougan, P.A. Williams, R.J. Skene, G. Snell, D. Scheibe, S. Kirby, D.J. Hosfield, D.E. Mcree, A.B. Schryvers, L.W. Tari, Crystal structure of *Pasteurella haemolytica* ferric ion-binding protein A reveals a novel class of bacterial iron-binding proteins, *J. Biol. Chem.* 278 (2003) 41093–41098.
- [16] S.R. Shouldice, R.J. Skene, D.R. Dougan, G. Snell, D.E. Mcree, A.B. Schryvers, L.W. Tari, Structural basis for iron binding and release by a novel class of periplasmic iron-binding proteins found in gram-negative pathogens, *J. Bacteriol.* 186 (2004) 3903–3910.
- [17] S.R. Shouldice, D.E. Mcree, D.R. Dougan, L.W. Tari, A.B. Schryvers, Novel anion-independent iron coordination by members of a third class of bacterial periplasmic ferric ion-binding proteins, *J. Biol. Chem.* 280 (2005) 5820–5827.

- [18] M. Guo, I. Harvey, W. Yang, L. Coghill, D.J. Campopiano, J.A. Parkinson, R.T. MacGillivray, W.R. Harris, P.J. Sadler, Synergistic anion and metal binding to the ferric ion-binding protein from *Neisseria gonorrhoeae*, *J. Biol. Chem.* 278 (2003) 2490–2502.
- [19] S.A. Tom-Yew, D.T. Cui, E.G. Bekker, M.E. Murphy, Anion-independent iron coordination by the *Campylobacter jejuni* ferric binding protein, *J. Biol. Chem.* 280 (2005) 9283–9290.
- [20] S.R. Shouldice, D.E. Mcrec, D.R. Dougan, L.W. Tari, A.B. Schryvers, Novel anion-independent iron coordination by members of a third class of bacterial periplasmic ferric ion-binding proteins, *J. Biol. Chem.* 280 (2005) 5820–5827.
- [21] P.A. Daskaleros, J.A. Stoebner, S.M. Payne, Iron uptake in *Plesiomonas shigelloides*: cloning of the genes for the heme-iron uptake system, *Infect. Immun.* 59 (1991) 2706–2711.
- [22] J.A. Stoebner, S.M. Payne, Iron-regulated hemolysin production and utilization of heme and hemoglobin by *Vibrio cholerae*, *Infect. Immun.* 56 (1988) 2891–2895.
- [23] C.L. Pickett, T. Auffenberg, E.C. Pesci, V.L. Sheen, S.S. Jusuf, Iron acquisition and hemolysin production by *Campylobacter jejuni*, *Infect. Immun.* 60 (1992) 3872–3877.
- [24] T. Lagergard, M. Purven, A. Frisk, Evidence of *Haemophilus ducreyi* adherence to and cytotoxic destruction of human epithelial cells, *Microb. Pathog.* 14 (1993) 417–431.
- [25] L.M. Simpson, J.D. Oliver, Regulation of proteolytic activity of *Vibrio vulnificus* by iron-containing compounds, *Microb. Pathog.* 14 (1993) 249–252.
- [26] B.R. Otto, S.J. van Dooren, J.H. Nuijens, J. Luirink, B. Oudega, Characterization of a hemoglobin protease secreted by the pathogenic *Escherichia coli* strain EB1, *J. Exp. Med.* 188 (1998) 1091–1103.
- [27] I.R. Henderson, F. Navarro-Garcia, J.P. Nataro, The great escape: structure and function of the autotransporter proteins, *Trends Microbiol.* 6 (1998) 370–378.
- [28] B.R. Otto, R. Sijbrandi, J. Luirink, B. Oudega, J.G. Heddle, K. Mizutani, S.Y. Park, J.R. Tame, Crystal structure of hemoglobin protease, a heme binding autotransporter protein from pathogenic *Escherichia coli*, *J. Biol. Chem.* 280 (2005) 17339–17345.
- [29] D. Perkins-Balding, M. Ratliff-Griffin, I. Stojiljkovic, Iron transport systems in *Neisseria meningitidis*, *Microbiol. Mol. Biol. Rev.* 68 (2004) 154–171.
- [30] C. Wandersman, P. Delepelaire, Bacterial iron sources: from siderophores to hemophores, *Annu. Rev. Microbiol.* 58 (2004) 611–647.
- [31] D. Perkins-Balding, A. Rasmussen, I. Stojiljkovic, Bacterial Heme and Hemoprotein Receptors, in: J.H. Crosa, A.R. Mey, S.M. Payne (Eds.), *Iron Transport in Bacteria*, ASM Press, Washington, 2004, pp. 66–85.
- [32] C.S. Bracken, M.T. Baer, A. Abdur-Rashid, W. Helms, I. Stojiljkovic, Use of heme-protein complexes by the *Yersinia enterocolitica* HemR receptor: histidine residues are essential for receptor function, *J. Bacteriol.* 181 (1999) 6063–6072.
- [33] L.A. Lewis, E. Gray, Y.P. Wang, B.A. Roe, D.W. Dyer, Molecular characterization of hpuAB, the haemoglobin-haptoglobin-utilization operon of *Neisseria meningitidis*, *Mol. Microbiol.* 23 (1997) 737–749.
- [34] K.H. Rohde, A.F. Gillaspay, M.D. Hatfield, L.A. Lewis, D.W. Dyer, Interactions of haemoglobin with the *Neisseria meningitidis* receptor HpuAB: the role of TonB and an intact proton motive force, *Mol. Microbiol.* 43 (2002) 335–354.
- [35] C.N. Cornelissen, P.F. Neisseria, Sparling, in: J.H. Crosa, A.R. Mey, S.M. Payne (Eds.), *Iron Transport in Bacteria*, ASM Press, Washington, 2004, pp. 256–272.
- [36] I. Stojiljkovic, V. Hwa, M.L. de Saint, P. O’Gaora, X. Nassif, F. Heffron, M. So, The *Neisseria meningitidis* haemoglobin receptor: its role in iron utilization and virulence, *Mol. Microbiol.* 15 (1995) 531–541.
- [37] I. Stojiljkovic, J. Larson, V. Hwa, S. Anic, M. So, HmbR outer membrane receptors of pathogenic *Neisseria* spp.: iron-regulated, hemoglobin-binding proteins with a high level of primary structure conservation, *J. Bacteriol.* 178 (1996) 4670–4678.
- [38] L.A. Lewis, D.W. Dyer, Identification of an iron-regulated outer membrane protein of *Neisseria meningitidis* involved in the utilization of hemoglobin complexed to haptoglobin, *J. Bacteriol.* 177 (1995) 1299–1306.
- [39] L.A. Lewis, M. Gipson, K. Hartman, T. Ownbey, J. Vaughn, D.W. Dyer, Phase variation of HpuAB and HmbR, two distinct haemoglobin receptors of *Neisseria meningitidis* DNM2, *Mol. Microbiol.* 32 (1999) 977–989.
- [40] S.K. Mazmanian, E.P. Skaar, A.H. Gaspar, M. Humayun, P. Gornicki, J. Jelenska, A. Joachimiak, D.M. Missiakas, O. Schneewind, Passage of heme-iron across the envelope of *Staphylococcus aureus*, *Science* 299 (2003) 906–909.
- [41] E.P. Skaar, O. Schneewind, Iron-regulated surface determinants (Isd) of *Staphylococcus aureus*: stealing iron from heme, *Microbes Infect.* 6 (2004) 390–397.
- [42] E.P. Skaar, A.H. Gaspar, O. Schneewind, IsdG and IsdI, heme-degrading enzymes in the cytoplasm of *Staphylococcus aureus*, *J. Biol. Chem.* 279 (2004) 436–443.
- [43] R.M. Pilpa, E.A. Fadeev, V.A. Villareal, M.L. Wong, M. Phillips, R.T. Clubb, Solution structure of the NEAT (NEAr Transporter) domain from IsdH/HarA: the human hemoglobin receptor in *Staphylococcus aureus*, *J. Mol. Biol.* 360 (2006) 435–447.
- [44] J.C. Grigg, C.L. Vermeiren, D.E. Heinrichs, M.E. Murphy, Haem recognition by a *Staphylococcus aureus* NEAT domain, *Mol. Microbiol.* 63 (2007) 139–149.
- [45] A.C. Chan, B. Leij-Garolla, I. Rosell, K.A. Pedersen, A.G. Mauk, M.E. Murphy, Cofacial heme binding is linked to dimerization by a bacterial heme transport protein, *J. Mol. Biol.* 362 (2006) 1108–1119.
- [46] D.P. Hildebrand, D.L. Burk, R. Maurus, J.C. Ferrer, G.D. Brayer, A.G. Mauk, The proximal ligand variant His93Tyr of horse heart myoglobin, *Biochemistry* 34 (1995) 1997–2005.
- [47] S. Eakanunkul, G.S. Lukat-Rodgers, S. Sumithran, A. Ghosh, K.R. Rodgers, J.H. Dawson, A. Wilks, Characterization of the periplasmic heme-binding protein shut from the heme uptake system of *Shigella dysenteriae*, *Biochemistry* 44 (2005) 13179–13191.
- [48] L. Debarbieux, C. Wandersman, Hemophore-Dependent Heme Acquisition Systems, in: J.H. Crosa, A.R. Mey, S.M. Payne (Eds.), *Iron Transport in Bacteria*, ASM Press, Washington, 2004, pp. 38–47.
- [49] S. Letoffe, J.M. Ghigo, C. Wandersman, Secretion of the *Serratia marcescens* HasA protein by an ABC transporter, *J. Bacteriol.* 176 (1994) 5372–5377.
- [50] N. Izadi, Y. Henry, J. Haladjian, M.E. Goldberg, C. Wandersman, M. Delepierre, A. Lecroisey, Purification and characterization of an extracellular heme-binding protein, HasA, involved in heme iron acquisition, *Biochemistry* 36 (1997) 7050–7057.
- [51] G. Kikuchi, T. Yoshida, M. Noguchi, Heme oxygenase and heme degradation, *Biochem. Biophys. Res. Commun.* 338 (2005) 558–567.
- [52] P. Arnoux, R. Haser, N. Izadi, A. Lecroisey, M. Delepierre, C. Wandersman, M. Czjzek, The crystal structure of HasA, a hemophore secreted by *Serratia marcescens*, *Nat. Struct. Biol.* 6 (1999) 516–520.
- [53] P. Arnoux, R. Haser, N. Izadi-Pruneyre, A. Lecroisey, M. Czjzek, Functional aspects of the heme bound hemophore HasA by structural analysis of various crystal forms, *Proteins* 41 (2000) 202–210.
- [54] S. Letoffe, C. Deniau, N. Wolff, E. Dassa, P. Delepelaire, A. Lecroisey, C. Wandersman, Hemophore-mediated bacterial haem transport: evidence for a common or overlapping site for haem-free and haem-loaded hemophore on its specific outer membrane receptor, *Mol. Microbiol.* 41 (2001) 439–450.
- [55] C. Deniau, R. Gilli, N. Izadi-Pruneyre, S. Letoffe, M. Delepierre, C. Wandersman, C. Briand, A. Lecroisey, Thermodynamics of heme binding to the HasA(SM) hemophore: effect of mutations at three key residues for heme uptake, *Biochemistry* 42 (2003) 10627–10633.
- [56] M. Czjzek, S. Letoffe, C. Wandersman, M. Delepierre, A. Lecroisey, N. Izadi-Pruneyre, The crystal structure of the secreted dimeric form of the hemophore HasA reveals a domain swapping with an exchanged heme ligand, *J. Mol. Biol.* 365 (2007) 1176–1186.
- [57] S. Letoffe, P. Delepelaire, C. Wandersman, Free and hemophore-bound heme acquisitions through the outer membrane receptor HasR have different requirements for the TonB–ExbB–ExbD complex, *J. Bacteriol.* 186 (2004) 4067–4074.

- [58] S. Letoffe, K. Wecker, M. Delepierre, P. Delepelaire, C. Wandersman, Activities of the *Serratia marcescens* heme receptor HasR and isolated plug and beta-barrel domains: the beta-barrel forms a heme-specific channel, *J. Bacteriol.* 187 (2005) 4637–4645.
- [59] N. Izadi-Pruneyre, F. Hucho, G.S. Lukat-Rodgers, A. Lecroisey, R. Gilli, K.R. Rodgers, C. Wandersman, P. Delepelaire, The heme transfer from the soluble HasA hemophore to its membrane-bound receptor HasR is driven by protein–protein interaction from a high to a lower affinity binding site, *J. Biol. Chem.* 281 (2006) 25541–25550.
- [60] F. Hucho, P. Delepelaire, C. Wandersman, W. Welte, Purification, crystallization and preliminary X-ray analysis of the outer membrane complex HasA–HasR from *Serratia marcescens*, *Acta Crystallogr. Sect. F. Struct. Biol. Cryst. Commun.* 62 (2006) 56–60.
- [61] H. Boukhalfa, A.L. Crumbliss, Chemical aspects of siderophore mediated iron transport, *BioMetals* 15 (2002) 325–339.
- [62] K.M. Raymond, E. Denz, Biochemical and Physical Properties of Siderophores, in: J.H. Crosa, A.R. Mey, S.M. Payne (Eds.), *Iron Transport in Bacteria*, ASM Press, Washington, 2004, pp. 3–17.
- [63] A.D. Ferguson, J. Koedding, G. Walker, C. Bos, J.W. Coulton, K. Diederichs, V. Braun, W. Welte, Active transport of an antibiotic rifamycin derivative by the outer-membrane protein FhuA, *Structure (Camb.)* 9 (2001) 707–716.
- [64] W.W. Yue, S. Grizot, S.K. Buchanan, Structural evidence for iron-free citrate and ferric citrate binding to the TonB-dependent outer membrane transporter FecA, *J. Mol. Biol.* 332 (2003) 353–368.
- [65] A.D. Ferguson, V. Braun, H.P. Fiedler, J.W. Coulton, K. Diederichs, W. Welte, Crystal structure of the antibiotic albomycin in complex with the outer membrane transporter FhuA, *Protein Sci.* 9 (2000) 956–963.
- [66] A.D. Ferguson, R. Chakraborty, B.S. Smith, L. Esser, H.D. van der, J. Deisenhofer, Structural basis of gating by the outer membrane transporter FecA, *Science* 295 (2002) 1715–1719.
- [67] A.D. Ferguson, E. Hofmann, J.W. Coulton, K. Diederichs, W. Welte, Siderophore-mediated iron transport: crystal structure of FhuA with bound lipopolysaccharide, *Science* 282 (1998) 2215–2220.
- [68] D.P. Chimento, R.J. Kadner, M.C. Wiener, Comparative structural analysis of TonB-dependent outer membrane transporters: implications for the transport cycle, *Proteins* 59 (2005) 240–251.
- [69] M. Struyve, M. Moons, J. Tommassen, Carboxy-terminal phenylalanine is essential for the correct assembly of a bacterial outer membrane protein, *J. Mol. Biol.* 218 (1991) 141–148.
- [70] A. Sauter, V. Braun, Defined inactive FecA derivatives mutated in functional domains of the outer membrane transport and signaling protein of *Escherichia coli* K-12, *J. Bacteriol.* 186 (2004) 5303–5310.
- [71] J.D. Faraldo-Gomez, G.R. Smith, M.S. Sansom, Molecular dynamics simulations of the bacterial outer membrane protein FhuA: a comparative study of the ferrichrome-free and bound states, *Biophys. J.* 85 (2003) 1406–1420.
- [72] K.P. Locher, B. Rees, R. Koebnik, A. Mitschler, L. Moulinier, J.P. Rosenbusch, D. Moras, Transmembrane signaling across the ligand-gated FhuA receptor: crystal structures of free and ferrichrome-bound states reveal allosteric changes, *Cell* 95 (1998) 771–778.
- [73] F. Endriss, V. Braun, Loop deletions indicate regions important for FhuA transport and receptor functions in *Escherichia coli*, *J. Bacteriol.* 186 (2004) 4818–4823.
- [74] D.P. Chimento, A.K. Mohanty, R.J. Kadner, M.C. Wiener, Substrate-induced transmembrane signaling in the cobalamin transporter BtuB, *Nat. Struct. Biol.* 10 (2003) 394–401.
- [75] C.A. Fuller-Schaefer, R.J. Kadner, Multiple extracellular loops contribute to substrate binding and transport by the *Escherichia coli* cobalamin transporter BtuB, *J. Bacteriol.* 187 (2005) 1732–1739.
- [76] S.K. Buchanan, B.S. Smith, L. Venkatramani, D. Xia, L. Esser, M. Palnitkar, R. Chakraborty, H.D. van der, J. Deisenhofer, Crystal structure of the outer membrane active transporter FepA from *Escherichia coli*, *Nat. Struct. Biol.* 6 (1999) 56–63.
- [77] D.C. Scott, Z. Cao, Z. Qi, M. Bauler, J.D. Igo, S.M. Newton, P.E. Klebba, Exchangeability of N termini in the ligand-gated porins of *Escherichia coli*, *J. Biol. Chem.* 276 (2001) 13025–13033.
- [78] G.E. Fanucci, J.Y. Lee, D.S. Cafiso, Spectroscopic evidence that osmolytes used in crystallization buffers inhibit a conformation change in a membrane protein, *Biochemistry* 42 (2003) 13106–13112.
- [79] D. Cobessi, H. Celia, N. Folschweiller, I.J. Schalk, M.A. Abdallah, F. Pattus, The crystal structure of the pyoverdine outer membrane receptor FpvA from *Pseudomonas aeruginosa* at 3.6 angstroms resolution, *J. Mol. Biol.* 347 (2005) 121–134.
- [80] D. Cobessi, H. Celia, F. Pattus, Crystal structure at high resolution of ferric-pyochelin and its membrane receptor FptA from *Pseudomonas aeruginosa*, *J. Mol. Biol.* 352 (2005) 893–904.
- [81] H.A. Eisenhauer, S. Shames, P.D. Pawelek, J.W. Coulton, Siderophore transport through *Escherichia coli* outer membrane receptor FhuA with disulfide-tethered cork and barrel domains, *J. Biol. Chem.* 280 (2005) 30574–30580.
- [82] D.P. Chimento, R.J. Kadner, M.C. Wiener, Comparative structural analysis of TonB-dependent outer membrane transporters: implications for the transport cycle, *Proteins* 59 (2005) 240–251.
- [83] J. Gumbart, M.C. Wiener, E. Tajkhorshid, Mechanics of force propagation in TonB-dependent outer membrane transport, *Biophys. J.* 93 (2007) 496–504.
- [84] L. Ma, W. Kaserer, R. Annamalai, D.C. Scott, B. Jin, X. Jiang, Q. Xiao, H. Maymani, L.M. Massis, L.C. Ferreira, S.M. Newton, P.E. Klebba, Evidence of ball-and-chain transport of ferric enterobactin through FepA, *J. Biol. Chem.* 282 (2007) 397–406.
- [85] V. Braun, M. Braun, H. Killmann, Ferrichrome- and Citrate-Mediated Iron Transport, in: J.H. Crosa, A.R. Mey, S.M. Payne (Eds.), *Iron Transport in Bacteria*, ASM Press, Washington, 2004, pp. 158–177.
- [86] V. Braun, S. Mahren, M. Ogierman, Regulation of the FecI-type ECF sigma factor by transmembrane signalling, *Curr. Opin. Microbiol.* 6 (2003) 173–180.
- [87] K. Poole, *Pseudomonas*, in: J.H. Crosa, A.R. Mey, S.M. Payne (Eds.), *Iron Transport in Bacteria*, ASM Press, Washington, 2004, pp. 293–310.
- [88] A. Garcia-Herrero, H.J. Vogel, Nuclear magnetic resonance solution structure of the periplasmic signalling domain of the TonB-dependent outer membrane transporter FecA from *Escherichia coli*, *Mol. Microbiol.* 58 (2005) 1226–1237.
- [89] A.D. Ferguson, C.A. Amezcua, N.M. Halabi, Y. Chelliah, M.K. Rosen, R. Ranganathan, J. Deisenhofer, Signal transduction pathway of TonB-dependent transporters, *Proc. Natl. Acad. Sci. U. S. A.* 104 (2007) 513–518.
- [90] C. Wirth, W. Meyer-Klaucke, F. Pattus, D. Cobessi, From the periplasmic signaling domain to the extracellular face of an outer membrane signal transducer of *Pseudomonas aeruginosa*: crystal structure of the ferric pyoverdine outer membrane receptor, *J. Mol. Biol.* 368 (2007) 398–406.
- [91] R. Tam, M.H. Saier Jr., Structural, functional, and evolutionary relationships among extracellular solute-binding receptors of bacteria, *Microbiol. Rev.* 57 (1993) 320–346.
- [92] J.P. Claverys, A new family of high-affinity ABC manganese and zinc permeases, *Res. Microbiol.* 152 (2001) 231–243.
- [93] Y.H. Lee, M.R. Dorwart, K.R.O. Hazlett, R.K. Deka, M.V. Norgard, J.D. Radolf, C.A. Hasemann, The crystal structure of Zn(II)-free *Treponema pallidum* TroA, a periplasmic metal-binding protein, reveals a closed conformation, *J. Bacteriol.* 184 (2002) 2300–2304.
- [94] Y.H. Lee, R.K. Deka, M.V. Norgard, J.D. Radolf, C.A. Hasemann, *Treponema pallidum* TroA is a periplasmic zinc-binding protein with a helical backbone, *Nat. Struct. Biol.* 6 (1999) 628–633.
- [95] M.C. Lawrence, P.A. Pilling, V.C. Epa, A.M. Berry, A.D. Ogunniyi, J.C. Paton, The crystal structure of pneumococcal surface antigen PsaA reveals a metal-binding site and a novel structure for a putative ABC-type binding protein, *Structure* 6 (1998) 1553–1561.
- [96] T.E. Clarke, S.Y. Ku, D.R. Dougan, H.J. Vogel, L.W. Tari, The structure of the ferric siderophore binding protein FhuD complexed with gallichrome, *Nat. Struct. Biol.* 7 (2000) 287–291.
- [97] T.E. Clarke, V. Braun, G. Winkelmann, L.W. Tari, H.J. Vogel, X-ray crystallographic structures of the *Escherichia coli* periplasmic protein FhuD bound to hydroxamate-type siderophores and the antibiotic albomycin, *J. Biol. Chem.* 277 (2002) 13966–13972.
- [98] A. Muller, A.J. Wilkinson, K.S. Wilson, A.K. Duhme-Klair, An [Fe

- (mecam)}2]6- bridge in the crystal structure of a ferric enterobactin binding protein, *Angew. Chem., Int. Ed. Engl.* 45 (2006) 5132–5136.
- [99] L. Holm, C. Sander, Protein-structure comparison by alignment of distance matrices, *J. Mol. Biol.* 233 (1993) 123–138.
- [100] E.L. Borths, K.P. Locher, A.T. Lee, D.C. Rees, The structure of *Escherichia coli* BtuF and binding to its cognate ATP binding cassette transporter, *Proc. Natl. Acad. Sci. U. S. A.* 99 (2002) 16642–16647.
- [101] N. Cadieux, C. Bradbeer, E. Reeger-Schneider, W. Koster, A.K. Mohanty, M.C. Wiener, R.J. Kadner, Identification of the periplasmic cobalamin-binding protein BtuF of *Escherichia coli*, *J. Bacteriol.* 184 (2002) 706–717.
- [102] N.K. Karpowich, H.H. Huang, P.C. Smith, J.F. Hunt, Crystal structures of the BtuF periplasmic-binding protein for vitamin B₁₂ suggest a functionally important reduction in protein mobility upon ligand binding, *J. Biol. Chem.* 278 (2003) 8429–8434.
- [103] K.D. Krewulak, C.M. Shepherd, H.J. Vogel, Molecular dynamics simulations of the periplasmic binding ferric-hydroxamate protein FhuD, *BioMetals* 18 (2005) 375–386.
- [104] C. Kandt, Z. Xu, D.P. Tieleman, Opening and closing motions in the periplasmic vitamin B₁₂ binding protein BtuF, *Biochemistry* 45 (2006) 13284–13292.
- [105] R.A. Larsen, M.G. Thomas, K. Postle, Protonmotive force, ExbB and ligand-bound FepA drive conformational changes in TonB, *Mol. Microbiol.* 31 (1999) 1809–1824.
- [106] A. Garcia-Herrero, R.S. Peacock, S. Howard, H.J. Vogel, The solution structure of the periplasmic domain of the TonB system ExbD reveals an unexpected homology with siderophore binding proteins, *Mol. Microbiol.* in press.
- [107] S. Konishi, S. Iwaki, T. Kimura-Someya, A. Yamaguchi, Cysteine-scanning mutagenesis around transmembrane segment VI of Tn10-encoded metal-tetracycline/H(+) antiporter, *FEBS Lett.* 461 (1999) 315–318.
- [108] M.F. Varela, C.E. Sansom, J.K. Griffith, Mutational analysis and molecular modelling of an amino acid sequence motif conserved in antiporters but not symporters in a transporter superfamily, *Mol. Membr. Biol.* 12 (1995) 313–319.
- [109] M.L. Aldema, L.M. McMurphy, A.R. Walmsley, S.B. Levy, Purification of the Tn10-specified tetracycline efflux antiporter TetA in a native state as a polyhistidine fusion protein, *Mol. Microbiol.* 19 (1996) 187–195.
- [110] J.C. Jaskula, T.E. Letain, S.K. Roof, J.T. Skare, K. Postle, Role of the TonB amino terminus in energy transduction between membranes, *J. Bacteriol.* 176 (1994) 2326–2338.
- [111] J.S. Evans, B.A. Levine, I.P. Trayer, C.J. Dorman, C.F. Higgins, Sequence-imposed structural constraints in the TonB protein of *E. coli*, *FEBS Lett.* 208 (1986) 211–216.
- [112] R.A. Larsen, G.E. Wood, K. Postle, The conserved proline-rich motif is not essential for energy transduction by *Escherichia coli* TonB protein, *Mol. Microbiol.* 10 (1993) 943–953.
- [113] N. Cadieux, R.J. Kadner, Site-directed disulfide bonding reveals an interaction site between energy-coupling protein TonB and BtuB, the outer membrane cobalamin transporter, *Proc. Natl. Acad. Sci. U. S. A.* 96 (1999) 10673–10678.
- [114] N. Cadieux, C. Bradbeer, R.J. Kadner, Sequence changes in the ton box region of BtuB affect its transport activities and interaction with TonB protein, *J. Bacteriol.* 182 (2000) 5954–5961.
- [115] R.S. Peacock, A.M. Weljie, H.S. Peter, F.D. Price, H.J. Vogel, The solution structure of the C-terminal domain of TonB and interaction studies with TonB box peptides, *J. Mol. Biol.* 345 (2005) 1185–1197.
- [116] R.S. Peacock, A. Andrushchenko, A.R. Demcoe, M. Gehmlich, L. Sia Lu, A. Garcia-Herrero, H.J. Vogel, Characterization of TonB interactions with the FepA cork domain and FecA N-terminal signaling domain, *BioMetals* 19 (2006) 127.
- [117] P.D. Pawelek, N. Croteau, C. Ng-Thow-Hing, C.M. Khursigara, N. Moiseeva, J.W. Coulton, Structure of TonB in complex with FhuA, *E. coli* outer membrane receptor, *Science* 312 (2007) 1399.
- [118] D.D. Shultis, M.D. Purdy, C.N. Banchs, M.C. Wiener, Outer membrane active transport: structure of the BtuB:TonB complex, *Science* 312 (2006) 1396–1399.
- [119] K. Gunter, V. Braun, In vivo evidence for FhuA outer membrane receptor interaction with the TonB inner membrane protein of *Escherichia coli*, *FEBS Lett.* 274 (1990) 85–88.
- [120] H. Schoffler, V. Braun, Transport across the outer membrane of *Escherichia coli* K12 via the FhuA receptor is regulated by the TonB protein of the cytoplasmic membrane, *Mol. Gen. Genet.* 217 (1989) 378–383.
- [121] D.M. Carter, I.R. Miousse, J.N. Gagnon, E. Martinez, A. Clements, J. Lee, M.A. Hancock, H. Gagnon, P.D. Pawelek, J.W. Coulton, Interactions between TonB from *Escherichia coli* and the periplasmic protein FhuD, *J. Biol. Chem.* 281 (2006) 35413–35424.
- [122] C. Chang, A. Mooser, A. Pluckthun, A. Wlodawer, Crystal structure of the dimeric C-terminal domain of TonB reveals a novel fold, *J. Biol. Chem.* 276 (2001) 27535–27540.
- [123] J. Koedding, P. Howard, L. Kaufmann, P. Polzer, A. Lustig, W. Welte, Dimerization of TonB is not essential for its binding to the outer membrane siderophore receptor FhuA of *Escherichia coli*, *J. Biol. Chem.* 279 (2004) 9978–9986.
- [124] J. Koedding, F. Killig, P. Polzer, S.P. Howard, K. Diederichs, W. Welte, Crystal structure of a 92-residue C-terminal fragment of TonB from *Escherichia coli* reveals significant conformational changes compared to structures of smaller TonB fragments, *J. Biol. Chem.* 280 (2005) 3022–3028.
- [125] Y. Liu, D. Eisenberg, 3D domain swapping: As domains continue to swap, *Protein Sci.* 11 (2002) 1285–1299.
- [126] J. Janin, C. Chothia, The structure of protein–protein recognition sites, *J. Biol. Chem.* 265 (1990) 16027–16030.
- [127] A. Sauter, S.P. Howard, V. Braun, In vivo evidence for TonB dimerization, *J. Bacteriol.* 185 (2003) 5747–5754.
- [128] J. Ghosh, K. Postle, Evidence for dynamic clustering of carboxy-terminal aromatic amino acids in TonB-dependent energy transduction, *Mol. Microbiol.* 51 (2004) 203–213.
- [129] J. Ghosh, K. Postle, Disulphide trapping of an in vivo energy-dependent conformation of *Escherichia coli* TonB protein, *Mol. Microbiol.* 55 (2005) 276–288.
- [130] K. Postle, R.A. Larsen, The TonB, ExbB, and ExbD Proteins, in: J.H. Crosa, A.R. Mey, S.M. Payne (Eds.), *Iron Transport in Bacteria*, ASM Press, 2004, pp. 96–112.
- [131] P.I. Higgs, R.A. Larsen, K. Postle, Quantification of known components of the *Escherichia coli* TonB energy transduction system: TonB, ExbB, ExbD and FepA, *Mol. Microbiol.* 44 (2002) 271–281.
- [132] K.P. Locher, A.T. Lee, D.C. Rees, The E-coli BtuCD structure: a framework for ABC transporter architecture and mechanism, *Science* 296 (2002) 1091–1098.
- [133] L.W. Hung, I.X. Wang, K. Nikaido, P.Q. Liu, G.F. Ames, S.H. Kim, Crystal structure of the ATP-binding subunit of an ABC transporter, *Nature* 396 (1998) 703–707.
- [134] J. Chen, G. Lu, J. Lin, A.L. Davidson, F.A. Quioco, A tweezers-like motion of the ATP-binding cassette dimer in an ABC transport cycle, *Mol. Cell* 12 (2003) 651–661.
- [135] K. Diederichs, J. Diez, G. Greller, C. Muller, J. Breed, C. Schnell, C. Vonrhein, W. Boos, W. Welte, Crystal structure of MalK, the ATPase subunit of the trehalose/maltose ABC transporter of the archaeon *Thermococcus litoralis*, *EMBO J.* 19 (2000) 5951–5961.
- [136] R. Gaudet, D.C. Wiley, Structure of the ABC ATPase domain of human TAP1, the transporter associated with antigen processing, *EMBO J.* 20 (2001) 4964–4972.
- [137] N. Karpowich, O. Martsinkevich, L. Millen, Y.R. Yuan, P.L. Dai, K. MacVey, P.J. Thomas, J.F. Hunt, Crystal structures of the MJ1267 ATP binding cassette reveal an induced-fit effect at the ATPase active site of an ABC transporter, *Structure* 9 (2001) 571–586.
- [138] Y.R. Yuan, S. Blecker, O. Martsinkevich, L. Millen, P.J. Thomas, J.F. Hunt, The crystal structure of the MJ0796 ATP-binding cassette. Implications for the structural consequences of ATP hydrolysis in the active site of an ABC transporter, *J. Biol. Chem.* 276 (2001) 32313–32321.
- [139] K.P. Hopfner, A. Karcher, D.S. Shin, L. Craig, L.M. Arthur, J.P. Carney, J.A. Tainer, Structural biology of Rad50 ATPase: ATP-driven conformational control in DNA double-strand break repair and the ABC-ATPase superfamily, *Cell* 101 (2000) 789–800.

- [140] G. Verdon, S.V. Albers, B.W. Dijkstra, A.J. Driessen, A.M. Thunnissen, Crystal structures of the ATPase subunit of the glucose ABC transporter from *Sulfolobus solfataricus*: nucleotide-free and nucleotide-bound conformations, *J. Mol. Biol.* 330 (2003) 343–358.
- [141] L. Schmitt, H. Benabdelhak, M.A. Blight, I.B. Holland, M.T. Stubbs, Crystal structure of the nucleotide-binding domain of the ABC-transporter haemolysin B: identification of a variable region within ABC helical domains, *J. Mol. Biol.* 330 (2003) 333–342.
- [142] H.A. Lewis, S.G. Buchanan, S.K. Burley, K. Connors, M. Dickey, M. Dorwart, R. Fowler, X. Gao, W.B. Guggino, W.A. Hendrickson, J.F. Hunt, M. C. Kearins, D. Lorimer, P.C. Maloney, K.W. Post, K.R. Rajashankar, M.E. Rutter, J.M. Sauder, S. Shriver, P.H. Thibodeau, P.J. Thomas, M. Zhang, X. Zhao, S. Emtage, Structure of nucleotide-binding domain 1 of the cystic fibrosis transmembrane conductance regulator, *EMBO J.* 23 (2004) 282–293.
- [143] E. Schneider, S. Hunke, ATP-binding-cassette (ABC) transport systems: functional and structural aspects of the ATP-hydrolyzing subunits/domains, *FEMS Microbiol. Rev.* 22 (1998) 1–20.
- [144] D.C. Gadsby, A.C. Naim, Control of CFTR channel gating by phosphorylation and nucleotide hydrolysis, *Physiol. Rev.* 79 (1999) S77–S107.
- [145] J. Zielinski, L.C. Tsui, Cystic fibrosis: genotypic and phenotypic variations, *Annu. Rev. Genet.* 29 (1995) 777–807.
- [146] K. Hollenstein, D.C. Frei, K.P. Locher, Structure of an ABC transporter in complex with its binding protein, *Nature* 446 (2007) 213–216.
- [147] J. Chen, S. Sharma, F.A. Quijoch, A.L. Davidson, Trapping the transition state of an ATP-binding cassette transporter: evidence for a concerted mechanism of maltose transport, *Proc. Natl. Acad. Sci. U. S. A.* 98 (2001) 1525–1530.
- [148] I.L. Urbatsch, B. Sankaran, P-glycoprotein is stably inhibited by vanadate-induced trapping of nucleotide at single catalytic site, *J. Biol. Chem.* 270 (1995) 19383–19390.
- [149] S. Sharma, A.L. Davidson, Vanadate-induced trapping of nucleotides by purified maltose transport requires ATP hydrolysis, *J. Bacteriol.* 182 (2000) 6570–6576.
- [150] T.J. Silhavy, S. Szmelcman, W. Boos, M. Schwartz, On the significance of the retention of ligand by protein, *Proc. Natl. Acad. Sci. U. S. A.* 72 (1975) 2120–2124.
- [151] E.O. Oloo, D.P. Tieleman, Conformational transitions induced by the binding of MgATP to the vitamin B₁₂ ATP-binding cassette (ABC) transporter BtuCD, *J. Biol. Chem.* 279 (2004) 45013–45019.
- [152] H.W. Pinkett, A.T. Lee, P. Lum, K.P. Locher, D.C. Rees, An inward-facing conformation of a putative metal-chelate-type ABC transporter, *Science* 315 (2007) 373–377.
- [153] D.C. Rees, A.T. Lee, E.L. Borths, K.P. Locher, Structure of BtuCD, the ABC transporter for vitamin B₁₂, *FASEB J.* 17 (2003) A1185.
- [154] A.H. Yang, R.T. MacGillivray, J. Chen, Y. Luo, Y. Wang, G.D. Brayer, A.B. Mason, R.C. Woodworth, M.E. Murphy, Crystal structures of two mutants (K206Q, H207E) of the N-lobe of human transferrin with increased affinity for iron, *Protein Sci.* 9 (2000) 49–52.
- [155] N.A. Peterson, V.L. Arcus, B.F. Anderson, J.W. Tweedie, G.B. Jameson, E.N. Baker, “Dilysine trigger” in transferrins probed by mutagenesis of lactoferrin: crystal structures of the R210G, R210E, and R210L mutants of human lactoferrin, *Biochemistry* 41 (2002) 14167–14175.
- [156] G. Kurisu, S.D. Zakharov, M.V. Zhalnina, S. Bano, V.Y. Eroukova, T.I. Rokitskaya, Y.N. Antonenko, M.C. Wiener, W.A. Cramer, The structure of BtuB with bound colicin E3 R-domain implies a translocon, *Nat. Struct. Biol.* 10 (2003) 948–954.
- [157] S.K. Buchanan, P. Lukacik, S. Grizot, R. Ghirlando, M.M. Ali, T.J. Barnard, K.S. Jakes, P.K. Kienker, L. Esser, Structure of colicin I receptor bound to the R-domain of colicin Ia: implications for protein import, *EMBO J.* 26 (2007) 2594–2604.
- [158] A.D. Ferguson, W. Welte, E. Hofmann, B. Lindner, O. Holst, J.W. Coulton, K. Diederichs, A conserved structural motif for lipopolysaccharide recognition by procaryotic and eucaryotic proteins, *Struct. Fold. Des.* 8 (2000) 585–592.
- [159] M.T. Sebulsky, B.H. Shilton, C.D. Speziali, D.E. Heinrichs, The role of FhuD2 in iron(III)-hydroxamate transport in *Staphylococcus aureus*. Demonstration that FhuD2 binds iron(III)-hydroxamates but with minimal conformational change and implication of mutations on transport, *J. Biol. Chem.* 278 (2003) 49890–49900.
- [160] R.N. Hvorup, B.A. Goetz, M. Niederer, K. Hollenstein, E. Perozo, K.P. Locher, Asymmetry in the structure of the ABC transporter-binding protein complex BtuCD-BtuF, *Science* 317 (2007) 1387–1390.